# CERAMIDE IN APOPTOSIS AND OXIDATIVE STRESS IN ALLERGIC INFLAMMATION AND ASTHMA

**Briana N. James BS[1], Clement Oyeniran PhD[1,2], Jamie L. Sturgill PhD[3], Jason Newton PhD[1,8], Rebecca Martin PhD[4], Erhard Bieberich PhD[5], Cynthia Weigel PhD[1], Melissa A. Maczis PhD[1], Elisa N. D. Palladino PhD[1], Joseph C. Lownik BS[4], John B. Trudeau BA[6], Joan M. Cook-Mills PhD[7], Sally Wenzel MD[6], Sheldon Milstien PhD[1], and Sarah Spiegel PhD[1]***

[1]Departments of Biochemistry and Molecular Biology and [4]Microbiology and Immunology, Virginia Commonwealth University School of Medicine, Richmond, VA, [3]Department of Internal Medicine, Division of Pulmonary, Critical Care, and Sleep Medicine and [5]Department of Physiology, University of Kentucky College of Medicine, Lexington, KY, [6]Department of Medicine, University of Pittsburgh, Pittsburgh, PA, [7]Department of Pediatrics, Herman B Wells Center for Pediatric Research, Indiana School of Medicine, Indianapolis, IN

***Corresponding author.** Dr. Sarah Spiegel, Department of Biochemistry and Molecular Biology and the Massey Cancer Center, Virginia Commonwealth University School of Medicine, PO Box 980614, Richmond, Virginia, 23298, Tel: +1-804-828-9330, E-mail: sarah.spiegel@vcuhealth.org

[2]Current address: Department of Microbial Infection and Immunity, The Ohio State University

[8]Current address: Department of Biology, Virginia Commonwealth University

Supported by National Institutes of Health Grant R01AI125433 (to S.S.).

**Disclosure of potential conflict of interest:** S. Spiegel received grants from the National Institutes of Health. The authors declare that they have no competing financial interests.

**Total Words:** 4127

This is the author's manuscript of the article published in final edited form as:

James, B. N., Oyeniran, C., Sturgill, J. L., Newton, J., Martin, R. K., Bieberich, E., Weigel, C., Maczis, M. A., Palladino, E. N. D., Lownik, J. C., Trudeau, J. B., Cook-Mills, J. M., Wenzel, S., Milstien, S., & Spiegel, S. (2020). Ceramide in apoptosis and oxidative stress in allergic inflammation and asthma. Journal of Allergy and Clinical Immunology. https://doi.org/10.1016/j.jaci.2020.10.024

## ABSTRACT

**Background:** Nothing is known about the mechanisms by which increased ceramide in the lung contributes to allergic responses and asthma severity.

**Objective:** We sought to investigate the functional role of ceramide in mouse models of allergic airway disease that recapitulate the cardinal clinical features of human allergic asthma.

**Methods:** Allergic airway disease was induced in mice by repeated intranasal administration of house dust mite or the fungal allergen *Alternaria alternata*. Processes that can be regulated by ceramide and are important for severity of allergic asthma were correlated with ceramide levels measured by mass spectrometry.

**Results:** Both allergens induced massive pulmonary apoptosis and also significantly increased reactive oxygen species in the lung. Prevention of increases in lung ceramide levels mitigated allergen-induced apoptosis, reactive oxygen species, and neutrophil infiltration. In contrast, dietary supplementation of the anti-oxidant α-tocopherol decreased reactive oxygen species but had no significant effects on ceramide elevation or apoptosis, indicating that the increases in lung ceramide levels in allergen-challenged mice are not mediated by oxidative stress. Moreover, specific ceramide species were altered in bronchoalveolar lavage fluid from patients with severe asthma compared to non-asthmatics.

**Conclusion:** Our data suggest that ceramide elevation after allergen challenge contributes to apoptosis, reactive oxygen species generation, and neutrophilic infiltrate that characterize the severe asthmatic phenotype. Ceramide might be the trigger of formation of Creola bodies found in the sputum of patients with severe asthma and

could be a biomarker to optimize diagnosis and to monitor and improve clinical outcomes in this disease.

**Capsule Summary**

The bioactive sphingolipid metabolite ceramide is increased in lungs of allergen-challenged mice and severe asthmatic patients, promotes apoptosis, oxidative stress and neutrophil recruitment that contribute to allergic asthma and correlates with asthma severity.

**Clinical Implications statement**

Our work suggests that allergen-induced ceramide elevation is the initial trigger of the apoptotic process leading to Creola body formation. Ceramide in bronchoalveolar lavage fluid has the potential to serve as a biomarker for specific asthma endotypes and disease severity.

**Key words:** asthma, ceramide, apoptosis, oxidative stress, biomarker.

**Abbreviations used:** AHR, airway hyperresponsiveness; Alt, *Alternaria alternata*; BALF, bronchoalveolar lavage fluid; CerS, ceramide synthase; GWAS, genome-wide association studies; FB1, fumonisin B1; HDM, house dust mite; LC-ESI-MS/MS, liquid chromatography–electrospray ionization–tandem mass spectrometry; Myr, myriocin; ORMDL3, ORM1 (yeast)-like protein 3; ROS, reactive oxygen species; SARP, Severe Asthma Research Program; SPT, serine palmitoyltransferase; S1P, sphingosine-1-phosphate; TUNEL, terminal deoxynucleotidyl transferase–mediated dUTP nick end-labeling.

## INTRODUCTION

More than 25 million Americans suffer from asthma, a chronic airway disease marked by airflow obstruction, airway hyperreactivity, and pulmonary inflammation. The heterogeneous nature of asthma complicates treatment options and hampers the development of a cure. However, over the years, extensive research has advanced understanding of the initiation and progression of this disease. There is a strong genetic component to asthma and numerous genome-wide association studies (GWAS) have identified ORM (yeast)-like protein isoform 3 (*ORMDL3*) as a gene associated with the onset of allergic asthma, the most common type [1-6]. ORMDL3 is one of 3 members of the mammalian ORMDL family proteins, which are endogenous negative regulators of serine palmitoyl transferase (SPT), the rate-limiting enzyme of the *de novo* sphingolipid biosynthesis pathway [7]. This evolutionarily conserved function of ORMDL3 as a regulator of sphingolipid synthesis instigated interest into how sphingolipids may be involved in the pathology of asthma. Intriguingly, we found that although physiologically, ORMDL3 is a negative regulator of ceramide *de novo* biosynthesis, highly elevated pathological ORMDL3 expression, such as observed in allergic asthma, enhanced ceramide levels primarily due to increased sphingolipid degradation in the salvage pathway [8]. Ceramide, the central metabolite of the sphingolipid pathway [9], is increased in lungs of guinea pigs by aerosol administration of ovalbumin [10] and in lungs of house dust mite (HDM) challenged mice [8]. Moreover, inhibition of ceramide production in the lung protected HDM challenged mice from inflammation and airway hyperreactivity [8]. In addition, intratracheal delivery of ceramide caused lung inflammation, tissue remodeling, and airway flow obstruction [11]. Because ceramide is a bioactive signaling

molecule involved in the regulation of several biological processes that may contribute to asthma [12, 13], these results led us to investigate the functional role of ceramide in mouse models of allergic airway disease that recapitulate the cardinal clinical features of human allergic asthma. Our data suggest that ceramide elevation after allergen challenge plays a key role in airway epithelial cell apoptosis, oxidative stress, and neutrophil infiltration, processes that amplify and contribute to asthma severity in mice and humans [14, 15]. Moreover, specific ceramide species were altered in bronchoalveolar lavage fluid (BALF) from severely asthmatic patients compared to non-asthmatics and correlated with airway neutrophilia, suggesting that ceramide has the potential to serve as a biomarker for specific asthma endotypes and disease severity.

## METHODS

### Mouse models of allergic asthma

Female C57BL/6J mice were obtained from Jackson Laboratories (Bar Harbor, ME) and housed in the animal care facilities at Virginia Commonwealth University under standard temperature, humidity, and timed light conditions and provided with standard rodent chow and water *ad libitum*. All animal protocols and procedures were approved by the Institutional Animal Care and Use Committee at Virginia Commonwealth University. In an acute HDM-dependent asthma model, eight-week-old mice were challenged intranasally (i.n.) with house dust mite (15 µg HDM/25 µL saline) from Greer Laboratories (Lenoir, NC; XPB70D3A2.5) or saline on days 1 - 5 and days 8 - 12, for a total of 10 challenges. To inhibit ceramide biosynthesis, thirty minutes before HDM challenge, mice were injected intraperitoneally (i.p,) with vehicle, myriocin (0.3 mg/kg), or FB1 (0.5 mg/kg) on days 10, 11, and 12. This route of administration was selected as

instilling these inhibitors directly to the lung induced massive damage and i.p. treatment with fumonisin B1 (FB1) and myriocin at these concentrations did not affect circulating lymphocytes [16].

In a HDM model of allergic asthma with a strong antigen-specific IgE response, female mice (8 weeks old) were immunized by an i.p. injection of HDM (50 µg in 100 µl saline) together with 100 µl of Imject alum on day 1. On days 15, 18, and 21, mice were challenged i.n. with HDM (25 µg in 25 µl saline).

For the fungal allergen model, mice were challenged i.n. with *Alternaria alternata* (25 µg Alt/25 µl saline) from Greer Laboratories (XPM1D3A2.5) on days 1, 4, 7, and 10.

**Tocopherol diet**

C57BL/6J mice were challenged intratracheally (i.t.) with HDM (10 µg/50 µl saline) or saline 3 times per week for a total of 6 or 8 challenges. During these challenges, mice were fed either an α-tocopherol-supplemented (250 mg/kg) diet or standard rodent chow diet. 24 h following the last challenge, lung tissue was collected [17].

**Assessment of airway function**

Mice were anesthetized with a mixture of ketamine (100 mg/kg), xylazine (10 mg/kg), and acepromazine (2 mg/kg) i.p. followed by insertion of an 18-guage cannula into the trachea and placement onto the FlexiVent apparatus (Scireq, Montreal, Canada). Ventilation was started and mice were injected i.p with the paralytic decamethonium bromide (0.5 mg). Airway hyperresponsiveness was measured in response to increasing doses of nebulized methacholine (0-100 mg/ml) as described [8].

Whole respiratory system resistance (R) was reported as calculated (cmH20/mL/sec) in the FlexiVent software version 8.0.4.

**Mass spectrometry measurements of sphingolipids**

Lipids were extracted from lung tissue and sphingolipids were quantified by liquid chromatography electrospray ionization-tandem mass spectrometry (LC-ESI-MS/MS), as previously described [8].

**Measurement of reactive oxygen species**

Reactive oxygen species (ROS) were measured in snap-frozen lung tissue homogenized in PBS using a general oxidative stress indicator [14]. Briefly, lung tissue homogenates were incubated with 0.04 mM CM-H2DCFDA (ThermoFisher) for 20 min at 37° C on a thermomixer (Eppendorf) and then centrifuged at 1400 rpm for 5 min at 4° C. Aliquots of the supernatants (50 µL) were placed in wells of a 96 well black bottom plate with clear bottoms (CELLSTAR). Fluorescence was measured with a TECAN infinite M1000 Pro plate reader at an excitation wavelength of 495 nm and emission wavelength of 527 nm and normalized to protein concentration measured with the BCA Protein Assay Kit (ThermoFisher).

**Clinical cohort and sample collection**

Asthmatic and healthy subjects were previously recruited to the Severe Asthma Research Program (SARP1-2), an NHLBI-funded study designed to characterize molecular, cellular, and physiological phenotypes of severe and non-severe asthmatics [18]. Details regarding SARP1 were described previously [19]. Subjects 13 years of age and older with asthma and healthy control subjects were recruited and American Thoracic Society guidelines were used to categorize subjects as severe (n = 10) or non-severe

asthma (n = 5) or healthy controls (n = 5) [20]. Control subjects were nonsmokers with no history of lung disease. BAL was performed with five 50 mL aliquots of saline, and BALF was recovered by hand suction. An aliquot of cell-free BALF supernatant (1 mL) stored at -80°C was shipped to VCU for sphingolipid analyses.

**Statistical analyses**

Statistical significances were determined with unpaired 2-tailed Student's t test for comparison of 2 groups, or by ANOVA for multiple comparisons using GraphPad Prism 7.0 software (San Diego, CA). For all experiments, the normality of each group was first checked with the Shapiro-Wilk statistical test. In case of non-normally distributed data, Mann Whitney or Kruskal-Wallis tests were done. Significance defined as *P < 0.05, **P < 0.01, and ***P < 0.001. Experiments were repeated three times with similar results. For clinical correlation analyses, Pearson's product-moment correlation (r) and the strength of the relationship (p-value) for BALF sphingolipid species and lung function and cell infiltration measurements were calculated and generated a correlation matrix plotted using Prism 7. Highly significant correlations were accepted for r>0.7 and r< -0.7 with P-values <0.05. For neutrophil populations, Spearman non-parametric correlations were determined.

BALF collection and analysis, isolation of primary lung alveolar epithelial cells, apoptosis determination with Annexin V and 7-AAD, measurement of ROS production by epithelial cells, neutrophil isolation and neutrophil attachment assays, immunocytochemistry and western blot analysis are detailed in the Methods section in this article's Online Repository.

**RESULTS**

**HDM challenge increases lung ceramide accompanied by increased apoptosis and ROS**

To examine the role of ceramide in allergic asthma, mice were sensitized with ten intranasal injections of HDM over the duration of two weeks. This acute model stimulates airway inflammation and hypersensitivity and excessive mucus production commonly observed in asthmatic patients [21, 22]. Consistent with previous studies [8, 23, 24], mice sensitized with HDM developed features of allergic asthma, including marked increase in BALF of eosinophils, as well as T and B cells and neutrophils to a lesser extent (Fig. 1A), and airway hyperresponsiveness (AHR) (Fig. 1B). Although a recent study suggested that HDM challenge did not affect ORMDL3 expression [25], in accordance with previous reports [8, 26, 27], we observed that HDM induced a robust increase in expression of ORMDL3 in lungs (Fig. 1C). As we [8] and others [25] reported previously, there was a significant increase in levels of multiple ceramide species with varying acyl chain lengths, particularly the predominant lung species C16:0, C24:0 and C24:1 in lungs of HDM challenged mice (Fig. 1D). However, levels of the major phosphatidylcholine 34:2 species were unaltered (Fig. 1E), suggesting that there was a specific increase in the bioactive sphingolipid metabolite ceramide.

To begin assessing the role of ceramide, we examined processes in which ceramide is known to play key roles, including apoptosis and generation of ROS [9, 28] that could contribute to allergic asthma [12, 13]. Exposure to allergens induces extensive damage and apoptosis of airway epithelium that are related to both chronicity and severity of asthma [29-31]. Indeed, Creola bodies, which are clusters of apoptotic lung epithelial cells, have long been described in the sputum of asthmatic patients [29, 32]. Yet

little is known of the initial trigger of the apoptotic process. In agreement with others [14, 33], we found that HDM challenge induced activation of caspase 3, the final executionary step preceding apoptosis, as measured by increased levels of cleaved caspase 3 in immunoblots (Fig. 1C). Increased apoptosis in the lungs of HDM challenged mice was also confirmed by immunohistochemical staining with antibody against cleaved caspase 3 (Fig. E1). Since elevated ceramides can increase ROS leading to apoptosis [9, 34], and it was shown that ROS and oxidative stress contribute to asthma pathology in mice and humans [14, 15], we next measured ROS production. HDM exposure increased lung ROS measured fluorometrically with CM-H2DCFDA (Fig. 1F).

Consistent with elevation of lung ceramide determined by mass spectrometry (Fig. 1D), lung sections from HDM-challenged mice but not saline treated mice also displayed increased staining with a specific anti-ceramide antibody [35] (Fig. 2A and Fig. E2). Lung cells with increased ceramide staining also showed increased co-staining for activated/cleaved caspase 3 (Fig. 2A), suggesting that ceramide may contribute to the increased apoptosis. Ceramide staining only partially co-localized with airway smooth muscle cells (Fig. E3). Importantly, increased ceramide and cleaved caspase-3 staining predominantly co-localized with cytokeratin 18, a marker for epithelial cells (Fig. 2B and Fig. E4), which are the first line of defense against inhaled allergens and are now recognized as important players in asthma pathogenesis [36].

**Lung ceramide, apoptosis, and ROS are increased in several mouse models of allergic asthma**

We next expanded our studies to examine effects of ceramide elevation, apoptosis, and ROS in other murine models of experimental asthma. In a model that

induces a strong antigen-specific IgE response and mast cell hyperplasia with moderate eosinophilia [37, 38], mice were sensitized i.p. with HDM in alum as an adjuvant and then challenged intranasally three times with HDM alone. Sensitization and challenges with HDM/alum induced AHR (Fig. 3A) with a significant increase in IgE and activation of mast cells (Fig. 3B and data not shown). In parallel, there was an increase in neutrophils and eosinophils in BALF (Fig. 3C). ORMDL3 expression was also increased (Fig. 3D), as well as many ceramide species (Fig. 3E). Concomitantly, caspase 3 activation (Fig. 3D) and generation of ROS (Fig. 3F) were also significantly increased.

To exclude HDM-dependent effects and to examine responses to other potent allergens, mice were exposed to the fungal extract of *Alternaria alternata*, another common allergen associated with allergic asthma disease [39]. As was reported previously [25, 27, 40], *Alternaria* induced the hallmark features of asthma in mice, including AHR, lung and airway inflammation, eosinophilia (Fig 3G,H), as well as increased ORMDL3 (Fig. 3I). In addition to increased ORMDL3, there was also significantly increased ceramide levels, particularly C16;0, C24:0, and C24:1 species, in the lungs of sensitized mice (Fig. 3J). Concurrently, caspase 3 cleavage (Fig 3I) and ROS were also increased compared to saline treated mice (Fig. 3K). Taken together, these results demonstrate that challenge with diverse allergens increases ceramide levels that correlate with induction of apoptosis and increased levels of ROS in the lung.

**Allergen induced ceramide and apoptosis is independent of ROS production**

The links between ceramide, ROS, and apoptosis are complex. On the one hand, increased ROS in the lung can lead to increased ceramide production and apoptosis [41, 42]. On the other hand, increased ceramide can lead to ROS production and apoptosis [34,

[42, 43]. Therefore, it was of interest to complete the elucidation of the sequence of events prevalent during allergic asthma and determine the effects of suppressing ROS production on ceramide and apoptosis. To this end, HDM-challenged mice were fed a normal diet supplemented with the anti-oxidant α-tocopherol, a vitamin E isoform that has been shown to decrease ROS *in vivo* and lung inflammation in response to HDM challenge [17, 44]. As expected, the α-tocopherol-supplemented diet significantly reduced lung ROS levels in HDM challenged mice compared to normal diet (Fig. 4A). In contrast, however, α-tocopherol supplementation did not decrease elevation of lung ceramide species induced by HDM challenge (Fig. 4B). Similarly, decreasing ROS production in these mice did not suppress apoptosis as measured by caspase 3 activation (Fig. 4C). These results suggest that allergen-induced increased ceramide and apoptosis are independent of its effects on ROS.

**Allergen-induced ROS and apoptosis is ceramide-dependent**

We have previously shown that treatment of HDM-challenged mice with the SPT inhibitor myriocin or fumonisin B1 (FB1), an inhibitor of ceramide synthases (CerS) (Fig. 5A), for the last 3 days of allergen challenge reduced lung ceramide levels and markedly suppressed AHR to methacholine [8]. Therefore, we examined whether preventing ceramide elevation affects apoptosis or ROS production. Indeed, i.p. treatment with myriocin 30 min prior to HDM challenges on days 10, 11, and 12, prevented elevation of all ceramide species in BALF (Fig. 5B), more potently than treatment with FB1. This data suggests that ceramide elevation is due to increased biosynthesis and salvage/recycling to a lesser extent**.** In agreement, dihydroceramides, precursors of ceramides and intermediates in its *de novo* biosynthesis, are also

increased in lung [8] and in BALF from HDM challenged mice and are decreased by these inhibitors (Fig. 5B)**.** Acidic sphingomyelinase, which cleaves sphingomyelin to ceramide, has been implicated in bronchial asthma in mice [45]. However, in contrast to significant increases in ceramides and dihydroceramides, sphingomyelin levels were essentially unchanged after exposure to HDM (Fig. E5), indicating that sphingomyelin degradation is not a major contributor to ceramide elevation. Interestingly, treatment with these inhibitors not only mitigated the increase in ceramides, they markedly reduced lung epithelial cell apoptosis induced by HDM as demonstrated by reduced TUNEL staining (Fig. 5C) and reduced caspase 3 cleavage in western blots (Fig. 5D) and also completely prevented ROS formation in the lung (Fig. 5E). These results suggest that allergen-induced apoptosis and ROS production in the lung are due to elevated ceramide.

To elucidate the direct effect of HDM and increased ceramide on apoptosis and ROS formation, primary lung epithelial cells were treated with HDM or D-erythro-C6-ceramide, which is converted in cells to endogenous C16- and C24-ceramide [46]. Both HDM and C6-ceramide reduced viable cells with an increase in both early and late apoptotic cells (defined as Annexin $V^+$) (Fig. E6A,B), as well as ROS generation, measured by fluorescence of intracellular oxidized DCF (Fig. E6C). FB1 inhibited apoptosis and ROS generation induced by HDM or C6-ceramide, whereas myriocin mitigated the effects of HDM but was less effective in C6-ceramide treated cells, consistent with the notion that generation of endogenous ceramides from short-chain ceramides requires deacylation and reacylation catalyzed by CerS [46]. These results suggest that, even in the absence of immune cells, HDM on its own can trigger

bronchial epithelial cell apoptosis and ROS generation in a ceramide-dependent manner.

**Levels of specific ceramide species associate with asthma severity in patients**

Next, it was of interest to determine whether ceramide levels were also increased in asthmatic patients. BALF is the most reliable specimen to examine the fluid lining of the lower respiratory tract and is often used for physiologically relevant asthma studies [47]. Therefore, sphingolipid profiles were determined in BALF from healthy controls and from asthmatic patients recruited from SARP1-2 [19] and classified by clinical activity as having no, mild, or severe disease. Relative to non-severe asthmatics, individuals with severe asthma had higher SARP Severity type scores. Spirometric measures of lung function including FEV1% and FVC% were lower in severe asthmatics than in non-severe asthmatics or healthy controls despite the usage of higher doses of inhaled corticosteroids and oral corticosteroids by severe asthmatics (Table I).

All ceramide species in BALF from severe asthmatics, except C18:1, were increased compared to healthy controls, with significant increases in C20, C26, and C26:1 ceramides (Fig. 6A). However, these increases in ceramide species were not observed in mild asthmatics. Somewhat unexpectedly, there were no significant differences in BALF levels of the bioactive sphingolipid metabolite sphingosine-1-phosphate (S1P) or the sphingoid bases, sphingosine and dihydrosphingosine, among the three groups (Fig. 6A).

Next, we examined whether changes of these ceramide species in the BALF correlated with lung function or immune cells infiltration. Several strong correlations were revealed by unbiased correlation matrix analysis (Fig. 6B). All ceramides with

different acyl chain lengths correlated with each other. Remarkably, there were also positive correlations between ceramides, particularly C16:0, C26:1, and C26:0, with the degree of neutrophil infiltration (Fig. 6BC). Moreover, these species also correlated with airway obstruction determined by FEV1pp and FEV1/FVC (Fig. 6C). Taken together, these data suggest that specific ceramide species correlate with markers of asthma severity and airway neutrophilia, which has been associated with asthma exacerbations that are refractory to corticosteroid treatment [48].

**Involvement of ceramide in HDM-induced recruitment of neutrophils into the lung**

We previously found that blocking ceramide elevation prevented AHR and decreased accumulation of eosinophils in HDM challenged mice [8]. Whereas type 2 eosinophilic inflammation is found in most asthmatics, a subset of patients has severe debilitating disease with neutrophil-predominant lung inflammation [48]. Because we found association in asthmatic patients between ceramide, asthma severity, and airway neutrophilia (Fig. 6B,C), it was of interest to examine the involvement of ceramides in aeroallergen-induced neutrophil recruitment into the lung. Immunofluorescence staining of lung sections with neutrophil-specific anti-Ly6G [49] revealed intense staining after HDM exposure, which was greatly reduced by treatment with myriocin or FB1 (Fig. 7A). Likewise, staining for myeloperoxidase (MPO), found predominantly in neutrophil granules and a marker of their activation, was increased by HDM and suppressed by the inhibitors of ceramide formation (Fig. 7A). Furthermore, consistent with a previous report [50], increasing lung ceramide by intranasal instillation of C16:0 ceramide, significantly increased numbers of neutrophils ($CD11b^{+}CD11c^{-}SiglecF^{-}Ly6G^{+}$) in the BALF (Fig. 7B).

To further examine whether increased ceramide in the epithelium triggers neutrophil recruitment, primary lung epithelial cells were treated for 20 h with HDM or D-erythro-C6-ceramide in the absence or presence of FB1 or myriocin to increase or suppress ceramide elevation, respectively. Treatment of primary lung epithelial cells with HDM or C6-ceramide increased neutrophil adhesion to the epithelial monolayer, which was reduced by myriocin or FB1 (Fig. 7C,D). Taken together, this data support a role for ceramide elevation in allergen-initiated lung neutrophil recruitment.

## Discussion

Exposure to airborne allergens such as HDM and *Alternaria alternata* are major causes of allergic asthma. The airway epithelium is the first line of defense of the lung and plays a key role in allergic sensitization and remodeling [36, 51]. These aeroallergens can also induce apoptosis and oxidative stress of the airway epithelium in mice, compromising its barrier function, increasing susceptibility to lung inflammation, leading to exacerbation of asthma [36]. However, the underlying mechanisms that trigger these events have not been fully elucidated. Here we demonstrated that HDM and *Alternaria* induced significant increases in the pro-apoptotic sphingolipid metabolite ceramide in bronchial epithelium. Prevention of ceramide elevation mitigated HDM-induced lung apoptosis, oxidative stress, and neutrophilia indicative of the critical role of ceramide in activating these processes. Importantly, pronounced reduction of AHR, eosinophils [8] and neutrophils in BALF, apoptosis, and oxidative stress was observed even when inhibitors of ceramide production were only administered during the late asthmatic responses. These observations provide direct evidence for the importance of ceramide in asthma-induced pathology.

Clusters of apoptotic bronchial epithelial cells, known as Creola bodies, have long been noted in the sputum of severe asthmatics [32, 52]. Creola bodies were detected in sputum of 60% of pediatric asthmatic patients, which correlated with mobilization into the airway of neutrophils but not eosinophils [29, 53]. Consistent with data from aeroallergen challenged mice [14, 54], there are several reports of apoptotic epithelial cells in endobronchial biopsies of adult patients with chronic, persistent asthma but not in biopsies from healthy volunteers [29-31, 55]. Based on our data, we speculate that ceramide elevation leading to caspase 3 activation, a crucial mediator of apoptosis, is the initial trigger of the apoptotic process leading to Creola body formation.

The recruitment and activation of neutrophils must be tightly regulated to balance their effector functions with their ability to damage tissues by release of proteases and ROS [56]. Our finding that allergen-driven airway neutrophilia was decreased by blocking ceramide elevation is important as neutrophilic inflammation in the asthmatic lung is associated with impaired lung function and more severe disease [48, 56, 57]. Ceramide treatment of neutrophils enhanced several pro-inflammatory pathways, including chemotaxis, phagocytosis, and neutrophil extracellular trap (NET) formation [58], a process by which neutrophils externalize web-like chromatin strands containing antimicrobial peptides, proteases, and cytotoxic enzymes [59]. Recently it was shown that NET formation is induced in allergic lung after exposure to an aeroallergen [59]. Thus, it is possible that elevation of ceramide we observed in the lung and BALF may also contribute to neutrophilic inflammation in severe asthma.

Allergic asthma is associated with increases in ROS that are critical for the initiation of inflammatory responses [60]. ROS levels are elevated in the lavage fluid of

asthmatic patients, likely produced by NADPH oxidase in immune cells infiltrating the lungs or by airway epithelial cells [61]. Markers of oxidative stress, including nitric oxide and 8-isoprostane, are elevated in exhaled breath condensate during asthma exacerbation and in patients with severe asthma [62]. Consistent with previous studies [14, 63], we observed that HDM and *Alternaria* challenges induced lung ROS generation. Moreover, inhibitors of ceramide generation also blocked ROS production in response to these aeroallergens. However, dietary supplementation of α-tocopherol, the isoform that contributes to the anti-oxidative and anti-inflammatory effects [17, 44], reduced HDM-induced ROS as expected, but had no effect on increases of ceramide or apoptosis. These data indicate that although lung oxidative stress is involved in airway inflammation [64], it is not the cause for allergen-induced ceramide generation or apoptosis that leads to extensive lung damage. Moreover, the α-tocopherol supplemented diet reduced AHR and eosinophil but not neutrophil infiltration [44], suggesting that an ROS-independent mechanism drives neutrophil recruitment. These results may also explain some of the inconsistent outcomes from clinical reports on the associations of vitamin E and asthma and its potential beneficial effects [65, 66].

Asthma is a very heterogeneous disease with multiple phenotypes and different onset, course, and treatment responses and there is a great need for biomarkers to improve diagnosis and treatment [67, 68]. Interestingly, our targeted sphingolipidomic analyses showed that specific ceramide acyl chain species, including C16, the predominant species, and particularly the very long chain C20, C26, and C26:1, were increased in BALF from severe asthmatic patients but not in mild asthmatics, whereas C18:1 was reduced in both mild and severe asthmatics. Somewhat surprisingly, S1P,

which has previously been implicated in allergic asthma [69, 70], was not significantly increased. These results support the physiological relevance of ceramide elevation in exacerbation of allergic asthma. An untargeted metabolomics analysis of serum from healthy individuals and asthmatics also found that increased levels of ceramide positively correlated with asthma severity [71]. However, the physiological relevance to asthma of changes in sphingolipids in the circulation is unclear.

The strengths of this study are that it represents carefully phenotyped asthmatic patients, eliminated self-reporting bias, contains extensive information on lung function and disease severity, and corticosteroid treatment. Thus an unbiased correlation matrix analysis revealed that these ceramide species significantly correlated with lung function, and intriguingly, strongly correlated with neutrophil infiltration. Increased airway neutrophil infiltration has been associated with asthma severity and asthma exacerbations [48, 57]. Neutrophilia also correlates with asthma that is refractory to corticosteroids, the mainstay of asthma treatment [48, 57]. Here, we have identified significant associations between increased levels of specific ceramide species in BALF with neutrophilic lung inflammation, asthma severity, and resistance to corticosteroids. Hence, these ceramide species could potentially identify endotypes for corticosteroid resistant severe asthma and also be biomarkers to optimize diagnosis and to monitor and improve clinical outcomes in asthma.

## ACKNOWLEDGMENTS

The authors thank Dr. Jeremy Allegood (Virginia Commonwealth University, Richmond, VA) for skillful sphingolipid analyses. This work was supported by NIH grant R01AI125433 (to S.S.). The fluorescence microscopy studies were supported by

R01NS095215 (to E.B.). J.S. was supported by Institutional Development Award P20GM103527. The authors acknowledge the Virginia Commonwealth University Lipidomics/Metabolomics, the Flow Cytometry and the Microscopy Shared resources, which are supported in part by funding from the NIH-NCI Cancer Center Support Grant P30 CA016059.

The authors declare no conflicts of interest.

**AUTHOR CONTRIBUTIONS**

B.N.J. contributed to the design of the study, writing of the manuscript, analysis of the data, administered allergen challenges for Figs. 1 and 2, and performed immunoblotting, and measured ROS for Figs. 1, 3, and 4. C.O. contributed to the analysis of the study and immunoblotting for Fig. 3 and carried out the experiments described in Fig. 7B. J.L.S. performed the allergen challenges and measured airway resistance for Fig. 3. J.N. measured ROS for Fig. 3 and contributed to the statistical analysis in Fig. 6. R.M. and J.C.L. performed the allergen challenges and measured airway resistance for Figs. 1 and 3A-C. E.B. performed all staining and microscopy for Figs. 2, E2 and E3. C.W. purified epithelial cells, carried out experiments in Figs. E6 and Fig. 7A-D. E.N.D.P. purified neutrophils. M.A.M. measured apoptosis for Fig. E6. Data from the asthma cohort described in Fig. 6 were provided by J.B.T. and S.W. J.M.C-M. provided the samples from the α-tocopherol diet/HDM experiment in Fig. 4. S.M. contributed to the analysis of data and writing of the manuscript. S.S. contributed to the conception and design of the study, analysis of data, and writing of the manuscript. All authors reviewed the results and approved the manuscript.

## REFERENCES


1. Moffatt MF, Kabesch M, Liang L, Dixon AL, Strachan D, Heath S, et al. Genetic variants regulating ORMDL3 expression contribute to the risk of childhood asthma. Nature 2007; 448:470-3.
2. Lluis A, Schedel M, Liu J, Illi S, Depner M, von Mutius E, et al. Asthma-associated polymorphisms in 17q21 influence cord blood ORMDL3 and GSDMA gene expression and IL-17 secretion. J. Allergy Clin. Immunol. 2011; 127:1587-94.
3. Schedel M, Michel S, Gaertner VD, Toncheva AA, Depner M, Binia A, et al. Polymorphisms related to ORMDL3 are associated with asthma susceptibility, alterations in transcriptional regulation of ORMDL3, and changes in T2 cytokine levels. J. Allergy Clin. Immunol. 2015; 136:893-903.
4. Stein MM, Thompson EE, Schoettler N, Helling BA, Magnaye KM, Stanhope C, et al. A decade of research on the 17q12-21 asthma locus: Piecing together the puzzle. J Allergy Clin Immunol 2018; 142:749-64 e3.
5. Schmiedel BJ, Seumois G, Samaniego-Castruita D, Cayford J, Schulten V, Chavez L, et al. 17q21 asthma-risk variants switch CTCF binding and regulate IL-2 production by T cells. Nat Commun 2016; 7:13426.
6. Kothari PH, Qiu W, Croteau-Chonka DC, Martinez FD, Liu AH, Lemanske RF, Jr., et al. Role of local CpG DNA methylation in mediating the 17q21 asthma susceptibility gasdermin B (GSDMB)/ORMDL sphingolipid biosynthesis regulator 3 (ORMDL3) expression quantitative trait locus. J Allergy Clin Immunol 2018; 141:2282-6 e6.
7. Breslow DK, Collins SR, Bodenmiller B, Aebersold R, Simons K, Shevchenko A, et al. Orm family proteins mediate sphingolipid homeostasis. Nature 2010; 463:1048-53.
8. Oyeniran C, Sturgill JL, Hait NC, Huang WC, Avni D, Maceyka M, et al. Aberrant ORM (yeast)-like protein isoform 3 (ORMDL3) expression dysregulates ceramide homeostasis in cells and ceramide exacerbates allergic asthma in mice. J. Allergy Clin. Immunol. 2015; 136:1035-46.
9. Hannun YA, Obeid LM. Sphingolipids and their metabolism in physiology and disease. Nat Rev Mol Cell Biol 2018; 19:175-91.
10. Masini E, Giannini L, Nistri S, Cinci L, Mastroianni R, Xu W, et al. Ceramide: a key signaling molecule in a Guinea pig model of allergic asthmatic response and airway inflammation. J. Pharmacol. Exp. Ther. 2008; 324:548-57.
11. Petrache I, Petrusca DN. The involvement of sphingolipids in chronic obstructive pulmonary diseases. Handb. Exp. Pharmacol. 2013; 216:247-64.
12. Sturgill JL. Sphingolipids and their enigmatic role in asthma. Adv Biol Regul 2018; 70:74-81.
13. James B, Milstien S, Spiegel S. ORMDL3 and allergic asthma: From physiology to pathology. J Allergy Clin Immunol 2019; 144:634-40.
14. Chan TK, Loh XY, Peh HY, Tan WN, Tan WS, Li N, et al. House dust mite-induced asthma causes oxidative damage and DNA double-strand breaks in the lungs. J Allergy Clin Immunol 2016; 138:84-96.

15. Brown SD, Baxter KM, Stephenson ST, Esper AM, Brown LA, Fitzpatrick AM. Airway TGF-beta1 and oxidant stress in children with severe asthma: association with airflow limitation. J. Allergy Clin. Immunol. 2012; 129:388-96.
16. Johnson VJ, He Q, Osuchowski MF, Sharma RP. Disruption of sphingolipid homeostasis by myriocin, a mycotoxin, reduces thymic and splenic T-lymphocyte populations. Toxicology 2004; 201:67-75.
17. Cook-Mills J, Gebretsadik T, Abdala-Valencia H, Green J, Larkin EK, Dupont WD, et al. Interaction of vitamin E isoforms on asthma and allergic airway disease. Thorax 2016; 71:954-6.
18. Moore WC, Evans MD, Bleecker ER, Busse WW, Calhoun WJ, Castro M, et al. Safety of investigative bronchoscopy in the Severe Asthma Research Program. J Allergy Clin Immunol 2011; 128:328-36 e3.
19. Peters MC, McGrath KW, Hawkins GA, Hastie AT, Levy BD, Israel E, et al. Plasma interleukin-6 concentrations, metabolic dysfunction, and asthma severity: a cross-sectional analysis of two cohorts. Lancet Respir Med 2016; 4:574-84.
20. Chung KF, Wenzel SE, Brozek JL, Bush A, Castro M, Sterk PJ, et al. International ERS/ATS guidelines on definition, evaluation and treatment of severe asthma. Eur Respir J 2014; 43:343-73.
21. Gregory LG, Lloyd CM. Orchestrating house dust mite-associated allergy in the lung. Trends Immunol. 2011; 32:402-11.
22. Plantinga M, Guilliams M, Vanheerswynghels M, Deswarte K, Branco-Madeira F, Toussaint W, et al. Conventional and monocyte-derived CD11b(+) dendritic cells initiate and maintain T helper 2 cell-mediated immunity to house dust mite allergen. Immunity 2013; 38:322-35.
23. Kool M, Willart MA, van Nimwegen M, Bergen I, Pouliot P, Virchow JC, et al. An unexpected role for uric acid as an inducer of T helper 2 cell immunity to inhaled antigens and inflammatory mediator of allergic asthma. Immunity 2011; 34:527-40.
24. Cyphert-Daly JM, Yang Z, Ingram JL, Tighe RM, Que LG. Physiologic response to chronic house dust mite exposure in mice is dependent on lot characteristics. J Allergy Clin Immunol 2019; 144:1428-32 e8.
25. Debeuf N, Zhakupova A, Steiner R, Van Gassen S, Deswarte K, Fayazpour F, et al. The ORMDL3 asthma susceptibility gene regulates systemic ceramide levels without altering key asthma features in mice. J Allergy Clin Immunol 2019.
26. Ha SG, Ge XN, Bahaie NS, Kang BN, Rao A, Rao SP, et al. ORMDL3 promotes eosinophil trafficking and activation via regulation of integrins and CD48. Nat. Commun. 2013; 4:1-9.
27. Miller M, Tam AB, Cho JY, Doherty TA, Pham A, Khorram N, et al. ORMDL3 is an inducible lung epithelial gene regulating metalloproteases, chemokines, OAS, and ATF6. Proc. Natl. Acad. Sci. U.S.A. 2012; 109:16648-53.
28. Maceyka M, Spiegel S. Sphingolipid metabolites in inflammatory disease. Nature 2014; 510:58-67.
29. White SR. Apoptosis and the airway epithelium. J. Allergy (Cairo) 2011; 2011:9484-6.
30. Zhou C, Yin G, Liu J, Liu X, Zhao S. Epithelial apoptosis and loss in airways of children with asthma. J Asthma 2011; 48:358-65.

31. Juncadella IJ, Kadl A, Sharma AK, Shim YM, Hochreiter-Hufford A, Borish L, et al. Apoptotic cell clearance by bronchial epithelial cells critically influences airway inflammation. Nature 2013; 493:547-51.
32. Yamada Y, Yoshihara S, Arisaka O. Creola bodies in wheezing infants predict the development of asthma. Pediatr. Allergy Immunol. 2004; 15:159-62.
33. Truong-Tran AQ, Ruffin RE, Foster PS, Koskinen AM, Coyle P, Philcox JC, et al. Altered zinc homeostasis and caspase-3 activity in murine allergic airway inflammation. Am J Respir Cell Mol Biol 2002; 27:286-96.
34. Garcia-Ruiz C, Colell A, Mari M, Morales A, Fernandez-Checa JC. Direct effect of ceramide on the mitochondrial electron transport chain leads to generation of reactive oxygen species. Role of mitochondrial glutathione. J Biol Chem 1997; 272:11369-77.
35. Krishnamurthy K, Dasgupta S, Bieberich E. Development and characterization of a novel anti-ceramide antibody. J Lipid Res 2007; 48:968-75.
36. Lambrecht BN, Hammad H. The airway epithelium in asthma. Nat. Med. 2012; 18:684-92.
37. Galli SJ, Tsai M. IgE and mast cells in allergic disease. Nat. Med. 2012; 18:693-704.
38. Maltby S, Tay HL, Yang M, Foster PS. Mouse models of severe asthma: Understanding the mechanisms of steroid resistance, tissue remodelling and disease exacerbation. Respirology 2017; 22:874-85.
39. Salo PM, Arbes SJ, Jr., Sever M, Jaramillo R, Cohn RD, London SJ, et al. Exposure to Alternaria alternata in US homes is associated with asthma symptoms. J Allergy Clin Immunol 2006; 118:892-8.
40. Loser S, Gregory LG, Zhang Y, Schaefer K, Walker SA, Buckley J, et al. Pulmonary ORMDL3 is critical for induction of Alternaria-induced allergic airways disease. J. Allergy Clin. Immunol. 2017; 139:1496-507 e3.
41. Castillo SS, Levy M, Thaikoottathil JV, Goldkorn T. Reactive nitrogen and oxygen species activate different sphingomyelinases to induce apoptosis in airway epithelial cells. Exp Cell Res 2007; 313:2680-6.
42. Lee J, Yeganeh B, Ermini L, Post M. Sphingolipids as cell fate regulators in lung development and disease. Apoptosis 2015; 20:740-57.
43. von Haefen C, Wieder T, Gillissen B, Starck L, Graupner V, Dorken B, et al. Ceramide induces mitochondrial activation and apoptosis via a Bax- dependent pathway in human carcinoma cells. Oncogene 2002; 21:4009-19.
44. Berdnikovs S, Abdala-Valencia H, McCary C, Somand M, Cole R, Garcia A, et al. Isoforms of vitamin E have opposing immunoregulatory functions during inflammation by regulating leukocyte recruitment. J Immunol 2009; 182:4395-405.
45. Boll S, Ziemann S, Ohl K, Klemm P, Rieg AD, Gulbins E, et al. Acid sphingomyelinase regulates TH 2 cytokine release and bronchial asthma. Allergy 2020; 75:603-15.
46. Ogretmen B, Pettus BJ, Rossi MJ, Wood R, Usta J, Szulc Z, et al. Biochemical mechanisms of the generation of endogenous long chain ceramide in response to exogenous short chain ceramide in the A549 human lung adenocarcinoma cell

line. Role for endogenous ceramide in mediating the action of exogenous ceramide. J. Biol. Chem. 2002; 277:12960-9.

47. Peters SP. Asthma phenotypes: nonallergic (intrinsic) asthma. J Allergy Clin Immunol Pract 2014; 2:650-2.
48. Ray A, Kolls JK. Neutrophilic Inflammation in Asthma and Association with Disease Severity. Trends Immunol 2017; 38:942-54.
49. Daley JM, Thomay AA, Connolly MD, Reichner JS, Albina JE. Use of Ly6G-specific monoclonal antibody to deplete neutrophils in mice. J Leukoc Biol 2008; 83:64-70.
50. Kamocki K, Van Demark M, Fisher A, Rush NI, Presson RG, Jr., Hubbard W, et al. RTP801 is required for ceramide-induced cell-specific death in the murine lung. Am. J. Respir. Cell Mol. Biol. 2013; 48:87-93.
51. Gandhi VD, Vliagoftis H. Airway epithelium interactions with aeroallergens: role of secreted cytokines and chemokines in innate immunity. Front Immunol 2015; 6:147.
52. Naylor B. The shedding of the mucosa of the bronchial tree in asthma. Thorax 1962; 17:69-72.
53. Yoshihara S, Yamada Y, Abe T, Linden A, Arisaka O. Association of epithelial damage and signs of neutrophil mobilization in the airways during acute exacerbations of paediatric asthma. Clin Exp Immunol 2006; 144:212-6.
54. Yuan X, Wang E, Xiao X, Wang J, Yang X, Yang P, et al. The role of IL-25 in the reduction of oxidative stress and the apoptosis of airway epithelial cells with specific immunotherapy in an asthma mouse model. Am J Transl Res 2017; 9:4137-48.
55. Trautmann A, Schmid-Grendelmeier P, Kruger K, Crameri R, Akdis M, Akkaya A, et al. T cells and eosinophils cooperate in the induction of bronchial epithelial cell apoptosis in asthma. J Allergy Clin Immunol 2002; 109:329-37.
56. Snelgrove RJ, Patel DF, Patel T, Lloyd CM. The enigmatic role of the neutrophil in asthma: Friend, foe or indifferent? Clin Exp Allergy 2018; 48:1275-85.
57. Panettieri RA, Jr. The Role of Neutrophils in Asthma. Immunol Allergy Clin North Am 2018; 38:629-38.
58. Corriden R, Hollands A, Olson J, Derieux J, Lopez J, Chang JT, et al. Tamoxifen augments the innate immune function of neutrophils through modulation of intracellular ceramide. Nat Commun 2015; 6:8369.
59. Krishnamoorthy N, Douda DN, Bruggemann TR, Ricklefs I, Duvall MG, Abdulnour RE, et al. Neutrophil cytoplasts induce TH17 differentiation and skew inflammation toward neutrophilia in severe asthma. Sci Immunol 2018; 3.
60. Qu J, Li Y, Zhong W, Gao P, Hu C. Recent developments in the role of reactive oxygen species in allergic asthma. J Thorac Dis 2017; 9:E32-E43.
61. Sahiner UM, Birben E, Erzurum S, Sackesen C, Kalayci O. Oxidative stress in asthma. World Allergy Organ J 2011; 4:151-8.
62. Kharitonov SA, Barnes PJ. Biomarkers of some pulmonary diseases in exhaled breath. Biomarkers 2002; 7:1-32.
63. Uchida M, Anderson EL, Squillace DL, Patil N, Maniak PJ, Iijima K, et al. Oxidative stress serves as a key checkpoint for IL-33 release by airway epithelium. Allergy 2017; 72:1521-31.

64. Auerbach A, Hernandez ML. The effect of environmental oxidative stress on airway inflammation. Curr Opin Allergy Clin Immunol 2012; 12:133-9.
65. Hoskins A, Roberts JL, 2nd, Milne G, Choi L, Dworski R. Natural-source d-alpha-tocopheryl acetate inhibits oxidant stress and modulates atopic asthma in humans in vivo. Allergy 2012; 67:676-82.
66. Pearson PJ, Lewis SA, Britton J, Fogarty A. Vitamin E supplements in asthma: a parallel group randomised placebo controlled trial. Thorax 2004; 59:652-6.
67. Wenzel SE. Asthma phenotypes: the evolution from clinical to molecular approaches. Nat. Med. 2012; 18:716-25.
68. Fajt ML, Wenzel SE. Asthma phenotypes and the use of biologic medications in asthma and allergic disease: the next steps toward personalized care. J Allergy Clin Immunol 2015; 135:299-310.
69. Rivera J, Proia RL, Olivera A. The alliance of sphingosine-1-phosphate and its receptors in immunity. Nat. Rev. Immunol. 2008; 8:753-63.
70. Price MM, Oskeritzian CA, Falanga YT, Harikumar KB, Allegood JC, Alvarez SE, et al. A specific sphingosine kinase 1 inhibitor attenuates airway hyperresponsiveness and inflammation in a mast cell-dependent murine model of allergic asthma. J. Allergy Clin. Immunol. 2013; 131:501-11.
71. Reinke SN, Gallart-Ayala H, Gomez C, Checa A, Fauland A, Naz S, et al. Metabolomics analysis identifies different metabotypes of asthma severity. Eur Respir J 2017; 49.

## FIGURE LEGENDS

**FIG 1. House dust mite challenge increases ceramide, apoptosis, and ROS in the lung.** (A-D) C57Bl/6J mice were sensitized and challenged intranasally with HDM or saline and lungs examined on day 15. (A) Inflammatory cells in BALF. (B) Airway resistance in response to increasing doses of nebulized methacholine was measured with the FlexiVent system. (C) Proteins in lung lysates were separated by SDS-PAGE and immunoblotted with the indicated antibodies. Blots were stripped and re-probed with anti-tubulin to show equal loading and transfer. (D,E) Lipids were extracted and (D) ceramide species and (E) phosphatidylcholine (PC, 34:2) measured by LC-ESI-MS/MS. (F) ROS was determined with CM-H2DCFDA and fluorescence measured. Data are mean ± SEM. A: n=4 and 5 mice/group; B, C: n=3 and 3, D-F: n=4 and 4 for saline and HDM, respectively. *P < 0.05, ***P < 0.001, compared to each saline control. Similar data were obtained in 2 additional experiments.

**FIG 2. Increased ceramide staining in HDM-challenged mice co-localizes with cleaved caspase 3 in lung epithelium. (A)** Mice were challenged i.n. with HDM or saline and lungs as indicated and examined on day 15 as described in Fig 1. Lung sections were stained with anti-ceramide antibody (red), anti-cleaved caspase 3 antibody (green). Lower panels are zoom boxes indicated in middle panels. (B) Lung sections were stained with anti-ceramide antibody (red), anti-cleaved caspase 3 antibody (green) and anti-cytokeratin 18 (yellow), a marker for epithelial cells. (A,B) All sections were co-stained with DAPI to visualize nuclei (blue). Co-localization is shown in the overlay panels. Size bar: 50 or 10 µm as indicated.

**FIG 3. Lung ceramide, apoptosis, and ROS are increased in different allergen-**

**driven asthma models.** (A-F) Mice were sensitized i.p. with HDM (50 µg HDM in alum), and then challenged i.n. on days 15, 18, and 21 with HDM (25 µg in saline) or saline alone as indicated, and lungs examined on day 24. (A) Airway resistance in response to increasing doses of nebulized methacholine was measured with the FlexiVent system. (B) Eosinophils and neutrophils in BALF. (C) Serum IgE levels. (D) Proteins in lung lysates were analyzed by immunoblotting with the indicated antibodies. Blots were stripped and re-probed with anti-tubulin to show equal loading and transfer. (E) Lipids were extracted and ceramide species were measured by LC-ESI-MS/MS. (F) ROS was measured fluorometrically. A: n=10 and 7; B: n=3 and 7; C: n=4 and 6; D: n=2 and 2; E,F: n=4 and 4, respectively. *P < 0.05, **P < 0.01 compared to each saline control. (G-K) Mice were challenged i.n. with *Alternaria alternata* (Alt, 25 µg) or saline on days 1, 4, 7, and 10. (G) On day 11, airway resistance in response to nebulized methacholine (12 mg/mL) was measured with the FlexiVent system. (H) Eosinophils and neutrophils in BALF. (I) Western blot analysis of ORMDL, total caspase 3, and cleaved caspase 3 expression in the lung. Tubulin was used as a loading control. (J) Lung ceramide species were measured by LC-ESI-MS/MS. (K) ROS was measured fluorometrically. Data are mean ± SD. G: n=4 and 3; H: n= 5 and 4; I, n= 3 and 3; J n=3 and 4; K: n= 6 and 3 respectively. *P < 0.05, **P < 0.01 compared to each saline control.

**FIG 4. Effects of feeding α-tocopherol supplemented diet on ROS, ceramide, and apoptosis in the lung of HDM challenged mice**. Mice fed chow diet without or with α-tocopherol (250 mg/kg) were challenged i.n. with HDM (10 µg in 50 µL saline) every other day for a total of 8 challenges. (A) ROS in lungs was determined fluorometrically by oxidation of 2,7-dichlorofluorescein. (B) Lung ceramide species were measured by

LC-ESI-MS/MS. (C) Western blot analysis of cleaved caspase 3 in the lung. A,B: n=4,4,4, and 4 respectively. *P < 0.05, **P < 0.01, ***P < 0.01 compared to saline.

**FIG 5. Inhibiting ceramide production decreases ROS and apoptosis induced by HDM**. (A-C) Mice were challenged daily intranasally with HDM or saline for 5 consecutive days from days 1 to 5 and from days 8 to 12. Mice were injected i.p. with vehicle, myriocin (Myr; 0.3 mg/kg), or fumonisin B1 (FB1, 0.5 mg/kg) 30 min prior to the HDM challenges on days 10, 11, and 12 and lungs were examined on day 15. (A) Scheme of ceramide formation by *de novo* biosynthesis and degradation. Myriocin inhibits SPT and FB1 inhibits ceramide synthases (CerS). (B) Sphingolipids were extracted from BALF and ceramide and dihydroceramide species measured by LC-ESI-MS/MS. (C) In situ TUNEL staining of lung sections. Size bars: 50 µm. (D) Western blot analysis of cleaved caspase 3 in the lung. (E) ROS was measured fluorometrically. Data are mean ± SD. B: n=4 for saline, 4 for HDM, 2 for saline+myriocin, 4 for HDM+myriocin; 2 for saline+FB1, 4 for HDM+FB1; D: n= 2,3 and 3 respectively; E: n=3 for saline, 7 for HDM, 2 for saline+myriocin, 3 for HDM+myriocin; 2 for saline+FB1, 4 for HDM+FB1. *P < 0.05, **P < 0.01 compared to each saline control.

**FIG 6. Association between asthma severity and ceramide species that are increased in BALF.** (A) Levels of ceramide species in BALF from healthy controls, non-severe asthmatics, and severe asthmatics described in Table I were measured by LC-ESI-MS/MS. * P < 0.05 compared to healthy controls. (B) Heat-map of matrix coefficient correlation of each ceramide species in the BALF and lung functions or immune cells infiltration. Visualization of the correlations between each pair of variables using product-moment coefficients. Stronger Pearson correlation coefficients (r) are

represented by black color. (C) Examples of correlations between C16 or C26:1 ceramides and neutrophils, and lung functions. Goodness of fit is indicated by $r^2$. Correlation of neutrophils with C16-ceramide (Spearman r = 0.3089 and P = 0.092) and with C26:1-ceramide (Spearman r=0.4141 and p = 0.039). Correlation of FEV1_FVC with C26:1-ceramide (Pearson r = 0.5548 and P = 0.01) and FEV1pp with C26:1-ceramide (Pearson r = 0.5742, and P =0.01 ).

**FIG 7. Increased ceramide in HDM-challenged mice enhances neutrophil recruitment to the lungs.** (A) Mice were challenged daily intranasally with HDM or saline for 5 consecutive days from days 1 to 5 and from days 8 to 12. Mice were injected i.p. with vehicle, myriocin (Myr; 0.3 mg/kg), or fumonisin B1 (FB1, 0.5 mg/kg) 30 min prior to the HDM challenges on days 10, 11, and 12 and lungs were examined on day 15 as described in Figure 5. Lung sections were stained with anti-Ly6G (red) or anti-MPO antibody (green) and co-stained with DAPI to visualize nuclei (blue). Size bar: 100 µm. (B,C) Primary lung epithelial cells incubated for 20 h with vehicle, D-erythro-C6-ceramide (C6-Cer, 1 µM), or HDM (100 µg/mL) in absence or presence of FB1 (1 µM) or myriocin (100 nM) as indicated. After extensive washing, purified labeled neutrophils were added for 4 h and adhesion assessed by fluorescence. (B) Following intranasal instillation of vehicle or C16:0 ceramide number of neutrophils in the BALF was determined by FACS. Data means ± SD. n = 8 and 10 mice/group, respectively. **P < 0.01. (C) Representative fluorescent images. (D) Data expressed as arbitrary fluorescence units are means ± SEM. n=5 for each group. Each sample represents an individual donor mouse. * p < 0.05 ** p < 0.01 compared to vehicle.

**Table I. Patient clinical characteristics and bronchiolar lavage cells**

| | Healthy Donors (HD) | Non-severe Asthma (NSA) | Severe Asthma (SA) |
|---|---|---|---|
| No. of subjects | 5 | 5 | 10 |
| **Clinical data** | | | |
| Age | 30.4 (23.2-51.8) | 32 (23.7-51) | 42 (22.4-59.5) |
| % Male | 20 | 20 | 30 |
| BMI | 24.2±5.7 (19.4-33.5) | 26.3±7.5 (18.6-40.2) | 30.3±4.1 (22.8-35.1) |
| **Lung function** | | | |
| SARP Severity | 1 | 3 | 4.4±0.5** (4-5) |
| FEV1 % predicted | 112±5.6 (107-121) | 84.6±19.2 (60-106) | 54.9±21** (21-83) |
| FVC % predicted | 110±6.3 (104-119) | 83.4±20.0 (56-104) | 63.0±23.8** (36.3-101) |
| FEV1/FVC | 0.85±0 (0.78-0.88) | 0.8±0.1 (0.73-0.87) | 0.6±0.08** (0.50-0.71) |
| Max FEV1 Reversal with BD | 4.47±3.5 (0.9-6.7) | 9.7±3.0 (6.9-14.7) | 33.5±24.7 (0-47.3) |
| **Medications** | | | |
| Oral steroids | NO | NO | YES |
| Inhaled corticosteroids | NO | YES | YES |
| High dose of inhaled corticosteroids | NO | NO | YES |
| **BALF leukocyte differentials** | | | |
| Total cell count (millions) | 8.2±2.5 (5.6-12) | 6.1±2.8 (2.0-9.4) | 4.87±3.4 (1-11.8) |
| Alveolar Macrophages (%) | 92.3±4.9 (86.3-97.7) | 84.6±9.1 (68.7-84.2) | 80.6±11.9 (48.3-91.6) |
| Neutrophils (%) | 0.9±1.3 (0-3.2) | 3.4±3.3 (1.9-10) | 6.6±8.9 (0.8-28.3) |
| Eosinophils (%) | 0.6±0.9 (0-2.1) | 1.2±1.4 (0-3.3) | 3.5±3.7 ( 0-11.3) |
| Lymphocytes (%) | 6.2±4.3 (2-12.7) | 10.8±7.6 (4-19) | 9.3±5.0 (3.8-21.7) |

Values represent the mean ± SD (range). BMI, body mass index; FEV1, forced expiratory volume in 1 second; FVC, forced vital capacity; BD, post-bronchodilator. ** $P < 0.01$ compared to healthy controls.

The authors have no conflicts of interest to declare.

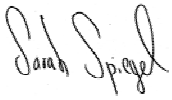

Sarah Spiegel, Ph.D.
Professor and Chair
Department of Biochemistry and Molecular Biology
Mann T. and Sara D. Lowry Chair in Cancer Research
VCU Massey Cancer Center

# CERAMIDE IN APOPTOSIS AND OXIDATIVE STRESS IN ALLERGIC INFLAMMATION AND ASTHMA

**Briana N. James BS[1], Clement Oyeniran PhD[1,2], Jamie L. Sturgill PhD[3], Jason Newton PhD[1], Rebecca Martin PhD[4], Erhard Bieberich PhD[5], Cynthia Weigel PhD[1], Melissa A. Maczis PhD[1], Elisa N. D. Palladino PhD[1], Joseph C Lownik BS[4], John B. Trudeau BA[6], Joan M. Cook-Mills PhD[7], Sally Wenzel MD[6], Sheldon Milstien PhD[1], and Sarah Spiegel PhD[1]*

## ONLINE REPOSITORY MATERIALS

## SUPPLEMENTARY METHODS

### BALF collection and analysis

BALF was collected by lavage of the lungs with 1 mL of PBS containing 1% BSA. Cellular composition of BALF was determined by fluorescence-activated cell sorting (FACS) as described [1, 2]. Briefly, cells stained with a fixable live/dead stain, Zombie Aqua (Biolegend) were incubated with Fc block anti-mouse CD16/CD32 (clone 2.4G2) in FACS buffer (2% BSA, 2mM ETDA, PBS) on ice for 10 min to reduce non-specific binding. Cells were then stained with an antibody cocktail (Supplementary Table 1) in FACS buffer and Brilliant Violet Stain Buffer (BD) according to the manufacturer's protocol. After staining and washing, cells were then fixed in 3% paraformaldehyde for 15 min at room temperature in the dark, washed, and re-suspended in PBS for analyses. Cells were run on a BD-LSRFORTESSA-X20 cell analyzer equipped with FACSDIVA 8.0 software for acquisition (BD Biosciences). Compensations were performed using single stain controls and negative controls with the assistance of UltraComp eBeads Plus compensation beads (ThermoFisher) to optimize fluorescence

compensation settings for multicolor flow cytometric analyses. Cells were first gated based on forward (FSC-A) and side (SSC-A) scatter to exclude debris and then were gated for doublet exclusion. All cells were gated as Fixable Zombie Aqua$^-$ (Live), and CD45$^+$. Unless otherwise noted, T cells were defined as CD3$^+$MHCII$^-$, B cells as B220$^+$CD19$^+$MHCII$^+$, macrophages as CD11c$^+$SiglecF$^+$, neutrophils as CD11b$^+$CD11c$^-$ SiglecF$^-$Gr1$^+$, and eosinophils as CD11c$^-$CD11b$^+$SiglecF$^+$SSC$^{high}$. Data analysis was performed using FlowJo version 10.4.2.

**Instillation of C16:0 ceramide**

C16:0 ceramide conjugated to polyethylene glycol 2000 (#880180P, Avanti Polar Lipids) dissolved in saline or vehicle was instilled intranasally (5 mg/kg) similar to a previous report with minor modifications [3]. After 24 h, BALF was collected and neutrophils (CD11b$^+$CD11c$^-$SiglecF$^-$Ly6G$^+$) quantified by FACS.

**Immunocytochemistry**

Frozen lung sections were fixed with 4% paraformaldehyde in PBS and permeabilized by incubation with 0.2% Triton X-100 in PBS for 5 min at room temperature. Nonspecific binding sites were blocked with 3% ovalbumin/10% donkey serum/PBS for 1 h at 37°C. Sections were then incubated with the indicated primary and secondary antibodies at a concentration of 5 µg/mL or 10 µg/mL in 0.1% ovalbumin as described previously [4]. Anti-ceramide rabbit IgG (1:200) was generated as previously described [5]. The anti-activated caspase 3 antibody (#9661, 1:400) was obtained from Cell Signaling Technology (Danvers, MA). The anti-cytokeratin-18 and anti-α-smooth muscle actin (SMA) (1:100) antibodies were from Santa Cruz (sc-398871 and sc-130616), anti-Ly6G was from BioLegend (clone 1A8, #127601) and anti-MPO antibody

from R&D Systems (#AF3667-SP). Cell nuclei were co-stained with 2 µg/mL DAPI in PBS for 30 min at room temperature. Paraffin lung sections were deparaffinated with xylene and ethanol, then microwave-irradiated and apoptotic cells were detected *in situ* with the Terminal deoxynucleotidyl transferase–mediated dUTP nick end-labeling (TUNEL) kit from Roche (Millipore Sigma). Epifluorescence microscopy was performed with a BZ-X810 Keyence fluorescence microscope or a Nikon Ti2 Eclipse microscope equipped with NIS Elements software using Z-scanning with 20x and 60x (oil) objective at the step size recommended by the software. Images were processed using the NIS Elements 3D deconvolution program at settings recommended by the software (automated) and deconvolved images were projected onto one plane. Laboratory personnel, blinded to the origin of the samples collected all of the data from at least three independent samples. Images obtained with secondary antibody only were used as negative controls.

**Isolation of primary lung alveolar epithelial cells**

Female C57BL/6J mice (8-12 weeks) were euthanized and perfused through the left ventricle with PBS supplemented with 0.1% heparin. The upper respiratory tract was exposed and the perfused lungs were dissected from the thoracic cavity and cut into single lobes. Tissues were placed in 15 mL conical tubes containing 5 mL of PBS with 0.5 mg/mL Liberase (Hoffmann-La Roche, Basel, Switzerland) and 0.02 mg/mL DNAse 1 (Sigma-Aldrich, St. Louis, Missouri, USA) and incubated for 30 min at 37 °C while shaking. Tissues were then dissociated mechanically and incubated further for 30 min. Digested tissues were passed through a 70 µm cell strainer and single cell suspensions centrifuged at 300 x g for 10 min at 4 °C. Cell pellets were re-suspended in 90 µl of PBS

containing 2 mM EDTA, 0.5% BSA, and 10 µl of CD326 (EpCAM) MicroBeads (Miltenyi Biotec, Bergisch Gladbach, Germany) per $10^7$ cells. After incubation for 15 min at 4°C, cells were re-suspended in 500 µl PBS containing 2 mM EDTA and 0.5% BSA. Labeled and non-labeled cells were separated by magnetic cell sorting with LS columns and the QuadroMACS separation system (Miltenyi Biotec, Bergisch Gladbach, Germany) according to the manufacturer´s instructions. The unlabeled flow-through was discarded and the labeled fractions were pelleted by centrifugation and re-suspended in 2 mL of in epithelial cell growth medium for animals EpiCM-A (ScienCell, San Diego, USA) at 500,000 cells/mL. Epithelial cells were cultured on poly-L-lysine-coated 6-well plates.

**Measurement of ROS production by epithelial cells**

Primary epithelial cells were plated and cultured to confluency in black 96 well plates with clear bottoms (Greiner Bio-One, Kremsmünster, Austria). Cells were then washed with PBS, and incubated with 100 µl of a 10 µM CM-$H_2$DCFA solution for 45 min at 37°C, 5% $CO_2$. The supernatants were removed and cells were washed twice with PBS and then stimulated for 24 h as described in figure legends. Fluorescence was measured with a TECAN infinite M1000 Pro fluorescence plate reader.

**Apoptosis determination with Annexin V and 7-amino-actinomycin D (7-AAD)**

Stimulated epithelial cells were harvested, including detached cells in the supernatant, and after centrifugation, cells were stained with the APC Annexin V Apoptosis Detection Kit with 7-AAD (BioLegend, San Diego, California, USA) according to the manufacturer´s instructions. Apoptosis was measured by flow cytometry using a BD LSRFortessa X-20 equipped with BD FACSDiva software for acquisition and

analysis (BD Biosciences, Franklin Lakes, New Jersey, USA). Data were analyzed using FlowJo 10.6.2 (FlowJo, LLC, Ashland, Oregon, USA).

**Neutrophil isolation and neutrophil attachment assay**

Primary neutrophils were isolated from lungs from female C57BL/6J mice by magnetic labeling of Ly-6G-positive cells. Briefly, mouse lungs were harvested and digested as described above. Single cell suspensions were centrifuged at 300 x g, 10 min, 4 °C, and the cell pellets re-suspended in 90 µl of PBS containing 2 mM EDTA, 0.5% BSA, and 10 µl of anti-Ly-6G MicroBeads (Miltenyi Biotec, Bergisch Gladbach, Germany) per $10^7$ cells. After incubation for 15 min at 4°C, the cells were re-suspended in 500 µl PBS containing 2 mM EDTA and 0.5% BSA, and separated by magnetic cell sorting with LS columns and the QuadroMACS separation system. The positive labeled cell fraction was centrifuged and re-suspended in 10 mL of 5 µM CellTrace CFSE dye (Invitrogen Molecular Probes, Eugene, Oregon, USA) in PBS. Cells were incubated for 15 min at 37°C and 40 mL of epithelial cell growth medium was added. After 5 min, cells were centrifuged for 5 min at 300 x g, 4 °C, and resuspended in epithelial cell growth medium at a cell density of 500,000 cells/mL. Primary epithelial cells were stimulated for 20 h as described in figure legends, and the supernatant was removed and replaced by 200 µl of the labeled neutrophil cell suspension. After 4 h, non-attached cells were carefully removed by three washes with PBS. During the last wash, the attached neutrophils were examined with the ZOE Fluorescent Cell Imager (Bio-Rad Laboratories, Hercules, California, USA). Cells were then lysed in 150 µl lysis buffer (50 mM NaCl solution with 10% SDS) for 5 min while shaking. 100 µL of the mixture was transferred to a black 96-well plate with clear bottom (Greiner Bio-One, Kremsmünster,

Austria). Fluorescence was measured at excitation and emission wavelengths of 492 and 517 nm with a TECAN Infinite M1000 fluorescence plate reader (Männedorf, Switzerland).

**Western blot analysis**

Snap frozen lung tissues were homogenized in buffer containing 50 mM Tris (pH 7.4), 150 mM NaCl, 1% NP-40, 2 mM sodium orthovanadate, 4 mM sodium pyrophosphate, 100 mM NaF, and 1:500 protease inhibitor mixture (Sigma). Equal amounts of protein were loaded and separated on 15% SDS-PAGE gels and transferred onto 0.45 µm nitrocellulose membranes using the PierceG2 Fast Blotter system (Thermo Scientific). 5% nonfat dry milk (BioRad) in TBS-T was used for blocking, and membranes were incubated with the following primary antibodies: anti-ORMDL3 (1:1000; CAT#ABN417, Millipore); anti-caspase 3 (1:1000; CAT#9662S, Cell Signaling); anti-cleaved capase 3 (1:1000; CAT#9664S, Cell Signaling); and anti-tubulin (1:20,000; CAT#2146S, Cell Signaling). Peroxidase-conjugated goat anti-rabbit secondary antibody (1:5000; Jackson ImmunoResearch) and chemiluminescent substrate (Pierce) were used to visualize protein bands.

**SUPPLEMENTARY REFERENCES**

1. Oyeniran C, Sturgill JL, Hait NC, Huang WC, Avni D, Maceyka M, et al. Aberrant ORM (yeast)-like protein isoform 3 (ORMDL3) expression dysregulates ceramide homeostasis in cells and ceramide exacerbates allergic asthma in mice. J. Allergy Clin. Immunol. 2015; 136:1035-46.

2. Lownik JC, Conrad DH, Martin RK. A Disintegrin and Metalloproteinase 17 is required for ILC2 responses to IL-33. Biochem Biophys Res Commun 2019; 512:723-8.

3. Kamocki K, Van Demark M, Fisher A, Rush NI, Presson RG, Jr., Hubbard W, et al. RTP801 is required for ceramide-induced cell-specific death in the murine lung. Am. J. Respir. Cell Mol. Biol. 2013; 48:87-93.

4. Jiang X, Zhu Z, Qin H, Tripathi P, Zhong L, Elsherbini A, et al. Visualization of Ceramide-Associated Proteins in Ceramide-Rich Platforms Using a Cross-Linkable Ceramide Analog and Proximity Ligation Assays With Anti-ceramide Antibody. Front Cell Dev Biol 2019; 7:166.

5. Krishnamurthy K, Dasgupta S, Bieberich E. Development and characterization of a novel anti-ceramide antibody. J Lipid Res 2007; 48:968-75.

## SUPPLEMENTARY FIGURE LEGENDS

**Figure E1. HDM induces lung apoptosis.** Mice were sensitized and challenged intranasally with HDM or saline and lung sections were stained with anti-cleaved caspase 3 antibodies. Bar: 100 µm.

**Figure E2.** Lack of autofluorescence of lung sections shown in Figure 2 stained with DAPI (blue).

**Figure E3. Increased lung ceramide by HDM partially co-localized with airway smooth muscle cells.** Mice were challenged i.n. with HDM or saline and lungs examined on day 15. Lung sections were stained with anti-ceramide antibody (red) and anti-SMA (green). All sections were co-stained with DAPI to visualize nuclei (blue). Co-localization is shown in the overlay panels. Bar: 50 µm.

**Figure E4. Increased ceramide staining in HDM-challenged mice co-localizes with cleaved caspase 3 and cytokeratin 18, marker for epithelial cells. (A)** Mice were challenged i.n. with HDM or saline and lungs as indicated and examined on day 15 as described in Fig 1. Lung sections were stained with anti-ceramide antibody, anti-cleaved caspase 3 antibody, anti-cytokeratin 18, and co-stained with DAPI. Co-localization is shown in the overlay panel. Size bar: 10 µm.

**Figure E5. HDM challenge increases BALF dihydro-ceramides and ceramides.** Mice were challenged daily i.n. with HDM or saline for 5 consecutive days from days 1 to 5 and from days 8 to 12. Mice were injected i.p. with vehicle, myriocin (Myr; 0.3 mg/kg), or fumonisin B1 (FB1, 0.5 mg/kg) 30 min prior to the HDM challenges on days 10, 11, and 12 and sphingolipids were extracted from BALF on day 15 and total levels of dihydroceramide (DH-Cer), monohexosyldihydroceramide (DH-HexCer),

dihydrosphingomyelin (DH-SM), ceramide (Cer), monohexosylceramide (HexCer), and sphingomyelin (SM) were measured by LC-ESI-MS/MS. n=4 and 7 respectively. Data are means ± SEM. *** $p < 0.001$ compared to saline.

**Figure E6. HDM induces apoptosis and ROS in lung epithelial cells in a ceramide-dependent manner.** (A) Representative flow cytometry analysis of primary lung epithelial cells treated with the vehicle or HDM (100 µg/mL) for 24 h followed by Annexin V and 7-AAD staining. (B,C) Primary lung epithelial cells were treated with vehicle, C6-ceramide (1 µM), HDM (100 µg/mL) in absence or presence of FB1 (1 µM), myriocin (100 nM) as indicated. (B) Cells were stained with Annexin V and 7-AAD and percent viable and apoptotic cells (Annexin $V^+$) determined by flow cytometry. (C) Increased ROS in cells was measured by oxidation of 2,7-dichlorofluorescein to fluorescent DCF. Data are means ± SD. B n=3 for each group; C: n=5 for each group. Each sample represents individual donor mouse.* $p < 0.05$ ** $p < 0.01$ compared to vehicle.

**Supplementary Table 1: Antibodies used**

| Target | Conjugate | Company | Clone | Product Number |
|---|---|---|---|---|
| Live/Dead | Zombie Aqua | Biolegend | | 423102 |
| CD45 | FITC | Biolegend | 30-F11 | 103108 |
| CD45 | APC-Fire750 | Biolegend | 30-F11 | 104154 |
| CD3e | BV711 | Biolegend | 145-2C11 | 100349 |
| CD3e | BUV737 | BD | 145-2C11 | 564618 |
| B220 | PE | Biolegend | RA3-6B2 | 103208 |
| B220 | BUV737 | BD | RA3-6B2 | 564449 |
| CD11b | PE/Cy7 | Biolegend | M1/70 | 101216 |
| CD11b | APC-Fire750 | Biolegend | M1/70 | 101262 |
| MHCII | BV421 | Biolegend | M5/114.15.2 | 107632 |
| MHCII | BV650 | Biolegend | M5/114.15.2 | 107641 |
| Gr1 | PE | Biolegend | RB6-8C5 | 108408 |
| Ly6G | FITC | Biolegend | 1A8 | 127606 |
| SiglecF | AF647 | BD | E50 2440 | 562680 |
| CD11c | BV605 | Biolegend | N418 | 117334 |
| CD11c | BV711 | Biolegend | N418 | 117349 |
| CD19 | PE/Cy7 | Biolegend | 6D5 | 115520 |

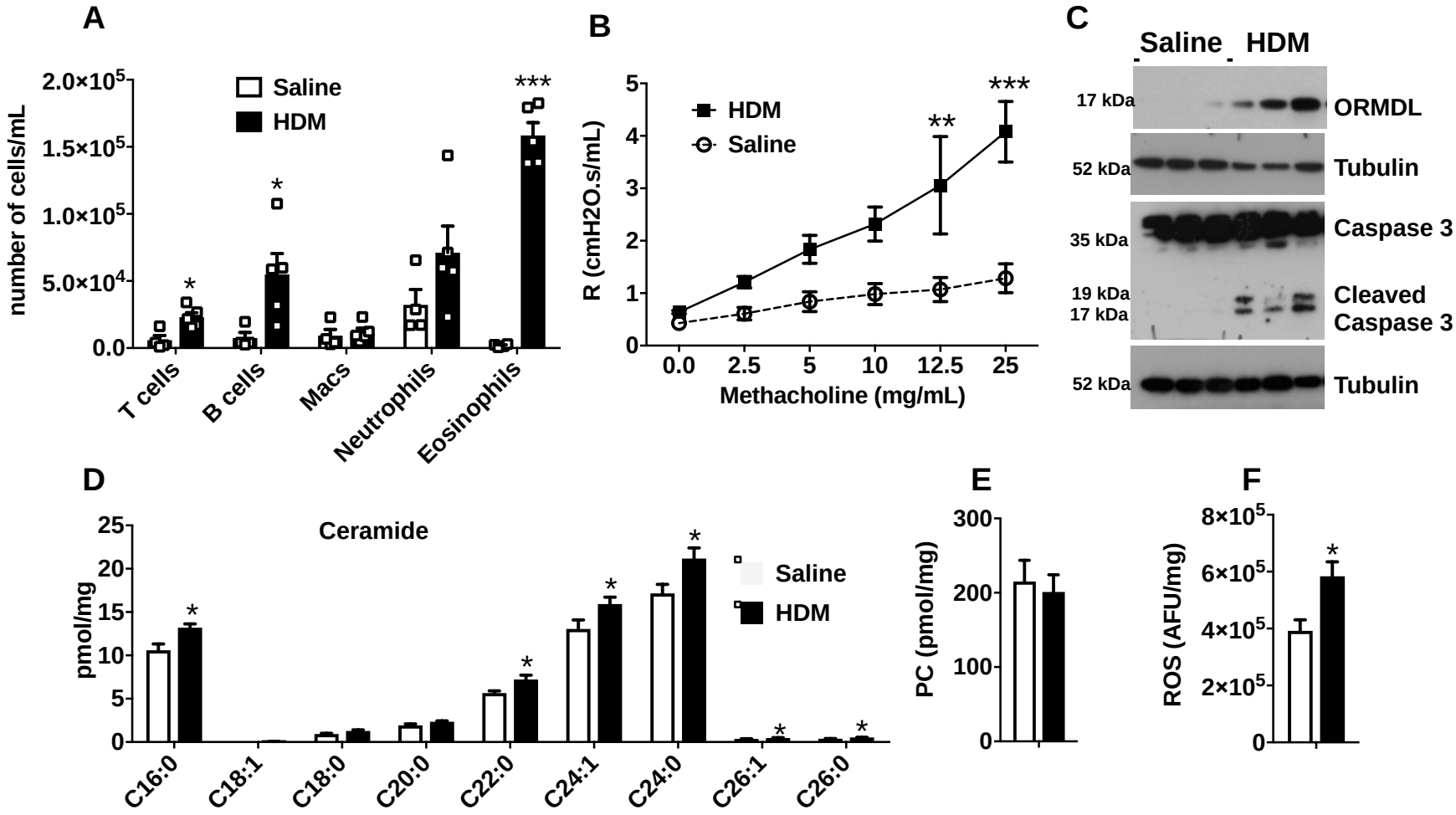
A
number of cells/mL
2.0×10^5
1.5×10^5
1.0×10^5
5.0×10^4
0.0
Saline
HDM
T cells
B cells
Macs
Neutrophils
Eosinophils
B
R (cmH2O.s/mL)
HDM
Saline
Methacholine (mg/mL)
0.0
2.5
5
10
12.5
25
C
Saline
HDM
17 kDa
ORMDL
52 kDa
Tubulin
35 kDa
Caspase 3
19 kDa
17 kDa
Cleaved Caspase 3
52 kDa
Tubulin
D
Ceramide
pmol/mg
Saline
HDM
C16:0
C18:1
C18:0
C20:0
C22:0
C24:1
C24:0
C26:1
C26:0
E
PC (pmol/mg)
F
ROS (AFU/mg)

Figure 1

Figure 2

A

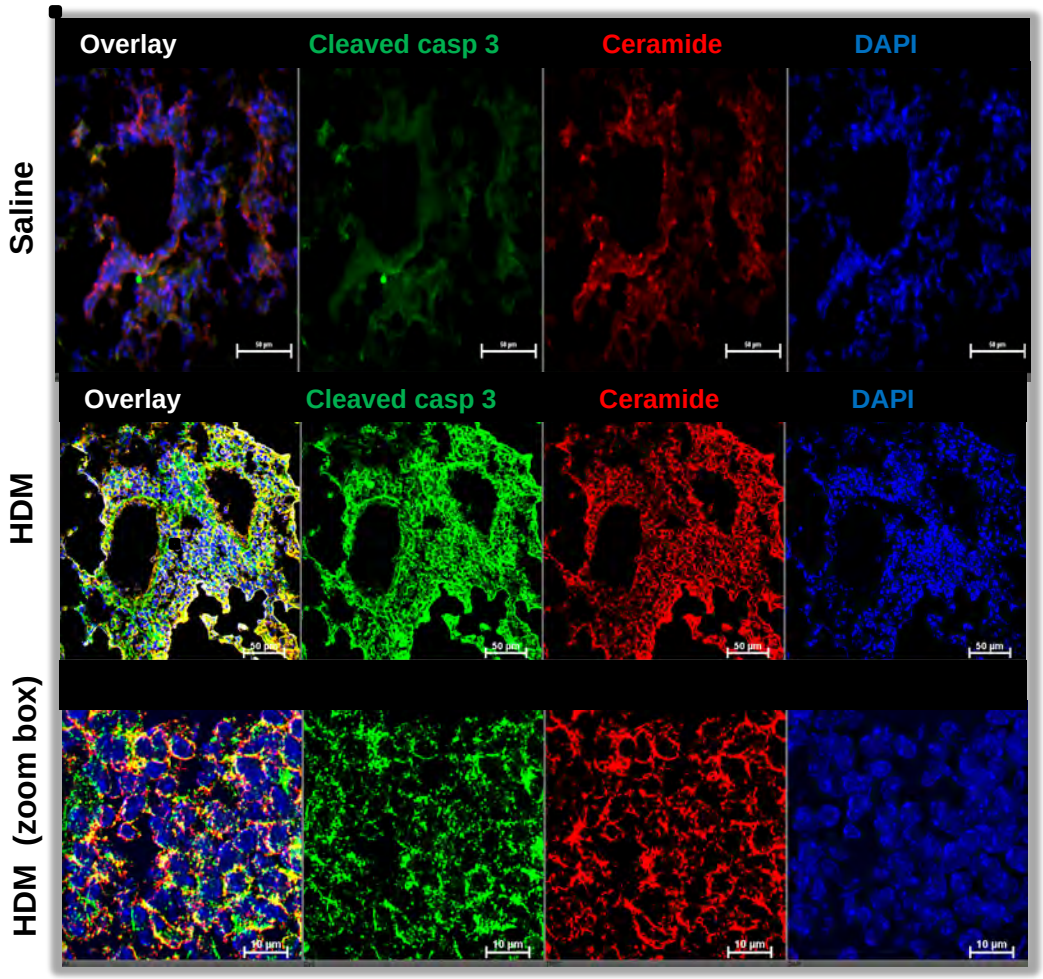
Overlay
Cleaved casp 3
Ceramide
DAPI
Saline
Overlay
Cleaved casp 3
Ceramide
DAPI
HDM
HDM (zoom box)

B

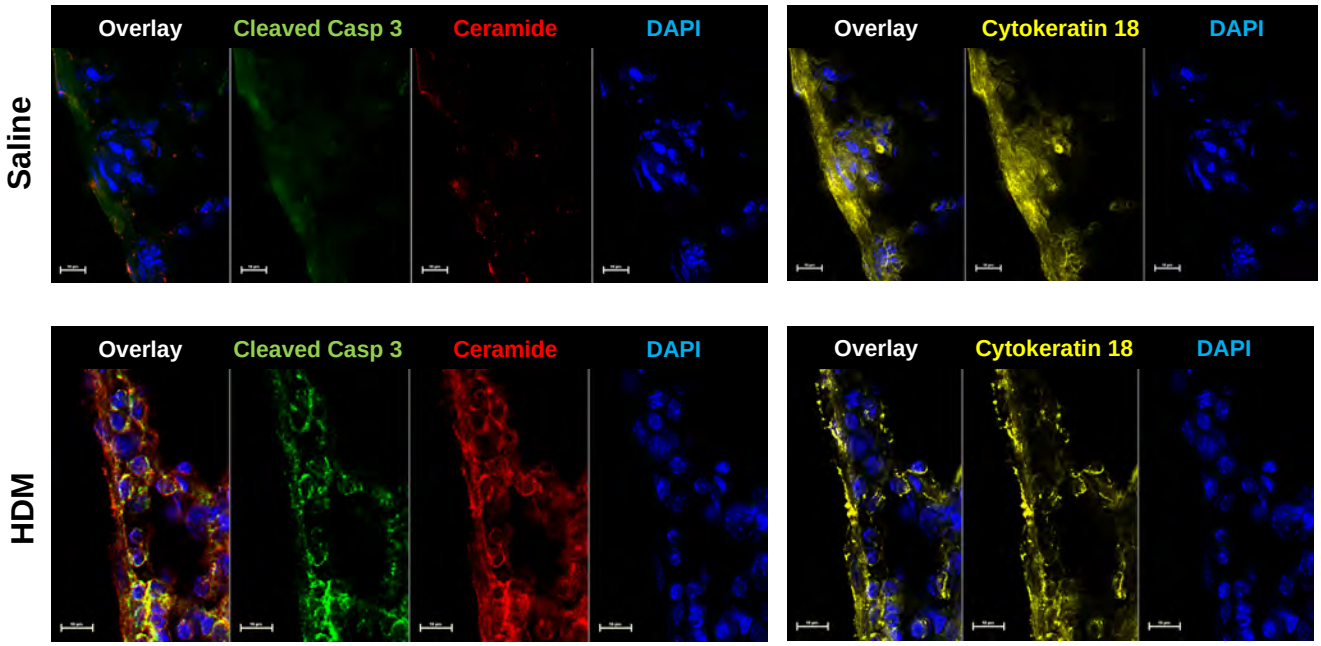
Overlay
Cleaved Casp 3
Ceramide
DAPI
Overlay
Cytokeratin 18
DAPI
Saline
Overlay
Cleaved Casp 3
Ceramide
DAPI
Overlay
Cytokeratin 18
DAPI
HDM

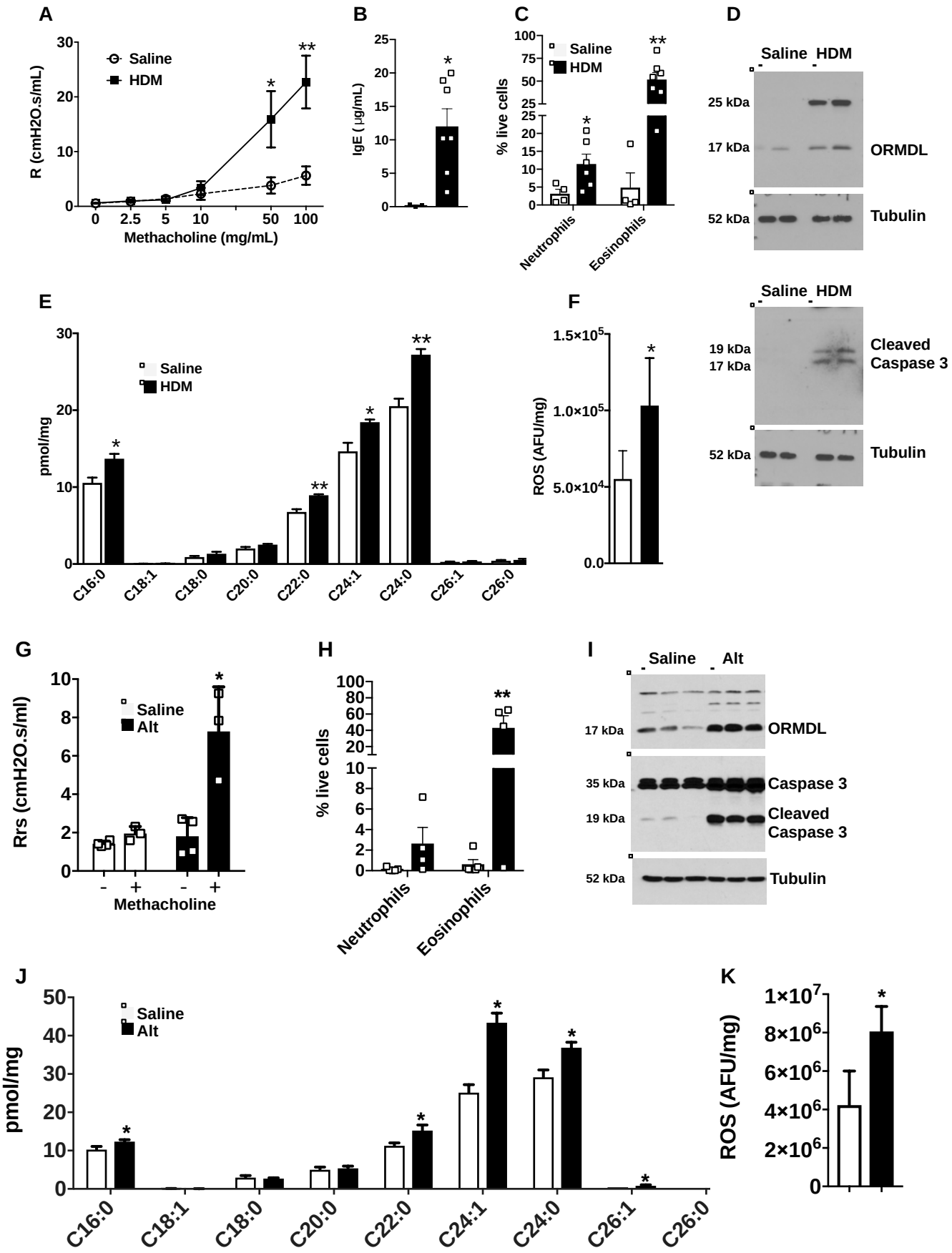
A
R (cmH2O.s/mL)
Saline
HDM
Methacholine (mg/mL)
B
IgE ( µg/mL)
C
% live cells
Saline
HDM
Neutrophils
Eosinophils
D
Saline HDM
25 kDa
17 kDa
ORMDL
52 kDa
Tubulin
E
pmol/mg
Saline
HDM
C16:0
C18:1
C18:0
C20:0
C22:0
C24:1
C24:0
C26:1
C26:0
F
ROS (AFU/mg)
Saline HDM
19 kDa
17 kDa
Cleaved Caspase 3
52 kDa
Tubulin
G
Rrs (cmH2O.s/ml)
Saline
Alt
Methacholine
H
% live cells
Neutrophils
Eosinophils
I
Saline Alt
17 kDa
ORMDL
35 kDa
Caspase 3
19 kDa
Cleaved Caspase 3
52 kDa
Tubulin
J
pmol/mg
Saline
Alt
C16:0
C18:1
C18:0
C20:0
C22:0
C24:1
C24:0
C26:1
C26:0
K
ROS (AFU/mg)

**Figure 3**

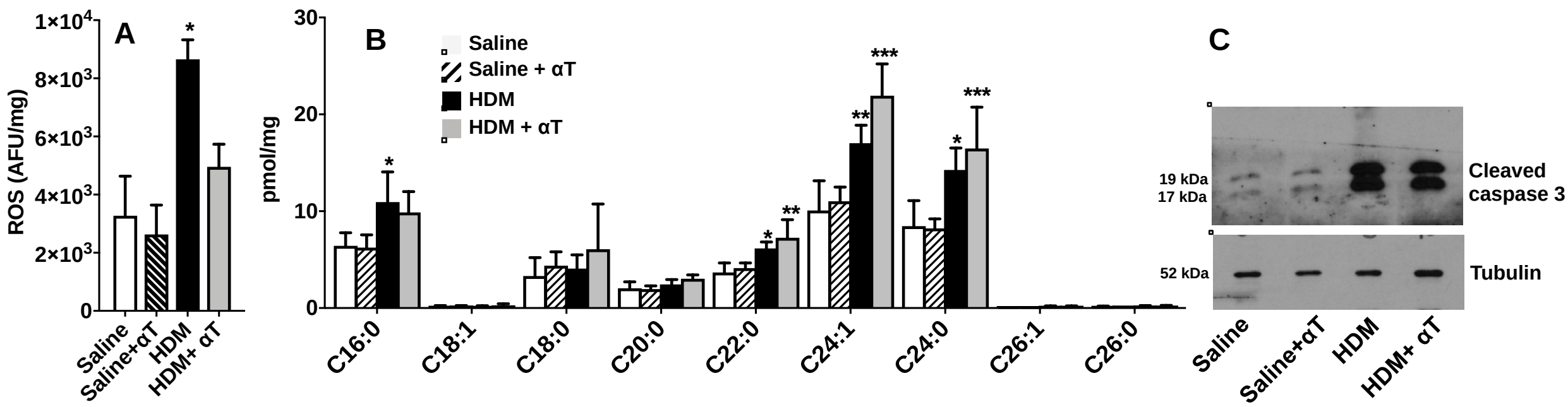
A
ROS (AFU/mg)
1×10^4
8×10^3
6×10^3
4×10^3
2×10^3
0
*
Saline
Saline+αT
HDM
HDM+ αT
B
pmol/mg
30
20
10
0
Saline
Saline + αT
HDM
HDM + αT
*
*
**
**
***
*
***
C16:0
C18:1
C18:0
C20:0
C22:0
C24:1
C24:0
C26:1
C26:0
C
19 kDa
17 kDa
Cleaved caspase 3
52 kDa
Tubulin
Saline
Saline+αT
HDM
HDM+ αT

Figure 4

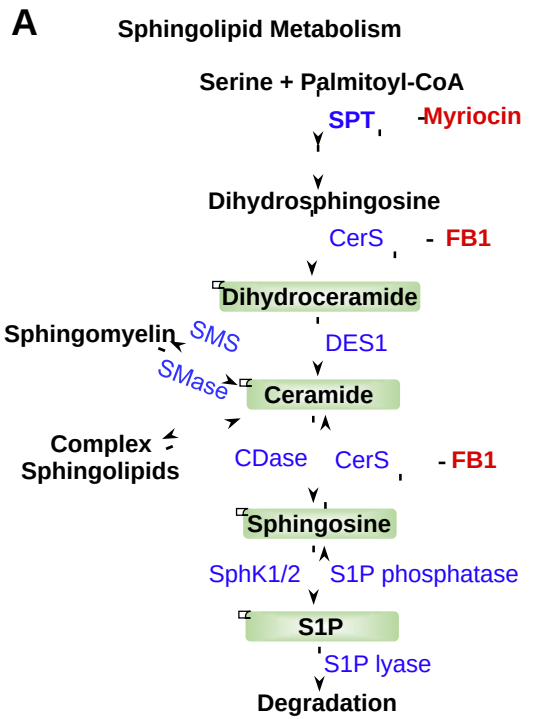
A
Sphingolipid Metabolism
Serine + Palmitoyl-CoA
SPT
-Myriocin
Dihydrosphingosine
CerS
- FB1
Dihydroceramide
Sphingomyelin
SMS
DES1
SMase
Ceramide
Complex Sphingolipids
CDase
CerS
- FB1
Sphingosine
SphK1/2
S1P phosphatase
S1P
S1P lyase
Degradation

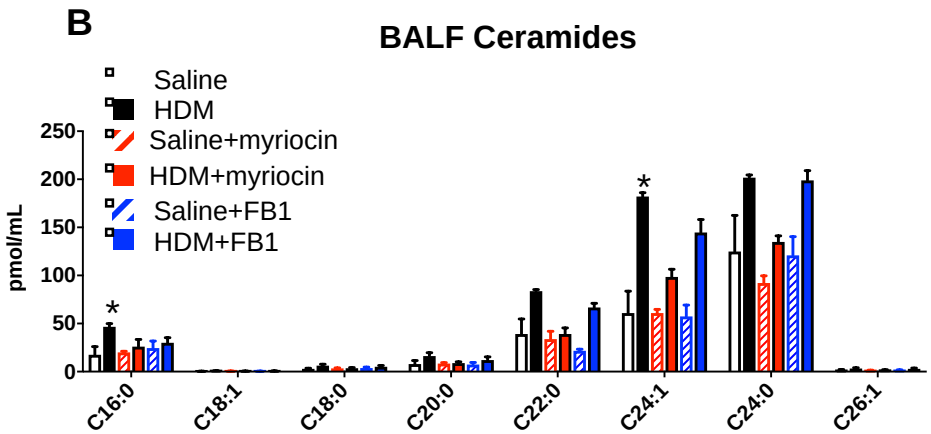
B
BALF Ceramides
Saline
HDM
Saline+myriocin
HDM+myriocin
Saline+FB1
HDM+FB1
pmol/mL
250
200
150
100
50
0
*
*
C16:0
C18:1
C18:0
C20:0
C22:0
C24:1
C24:0
C26:1

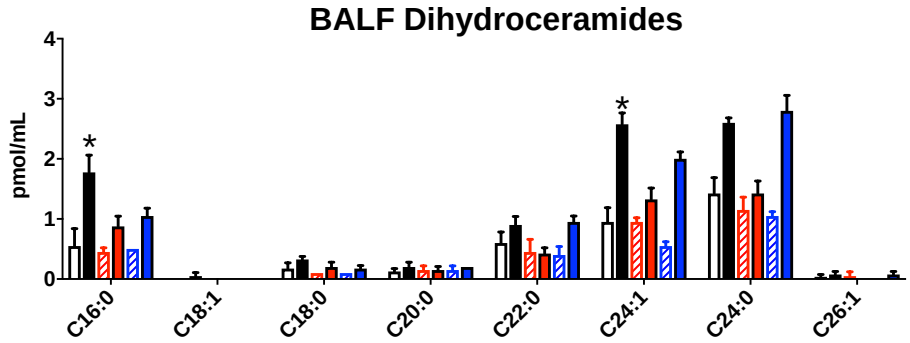
BALF Dihydroceramides
pmol/mL
4
3
2
1
0
*
*
C16:0
C18:1
C18:0
C20:0
C22:0
C24:1
C24:0
C26:1

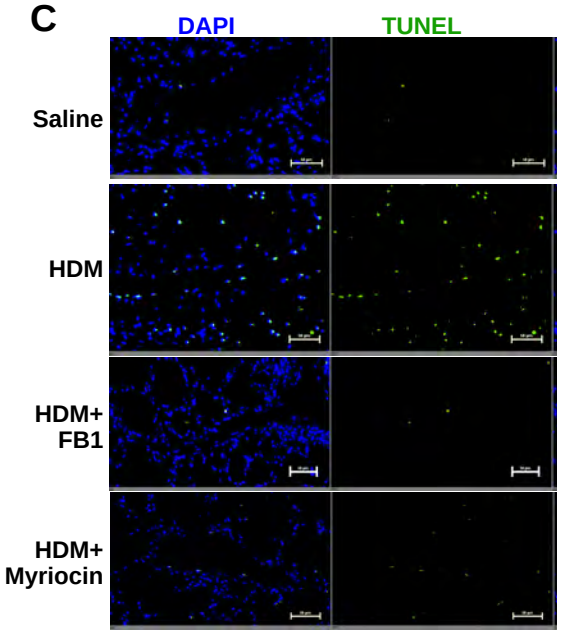
C
DAPI
TUNEL
Saline
HDM
HDM+ FB1
HDM+ Myriocin

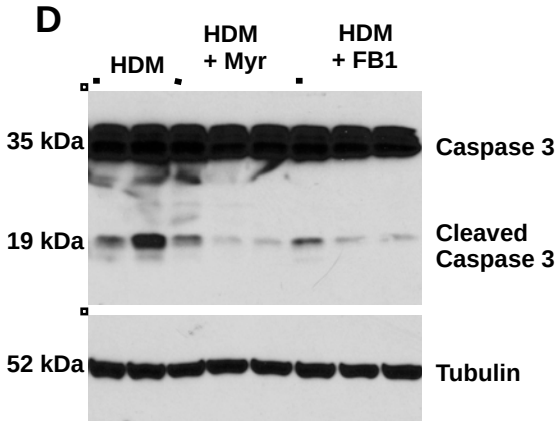
D
HDM
HDM + Myr
HDM + FB1
35 kDa
Caspase 3
19 kDa
Cleaved Caspase 3
52 kDa
Tubulin

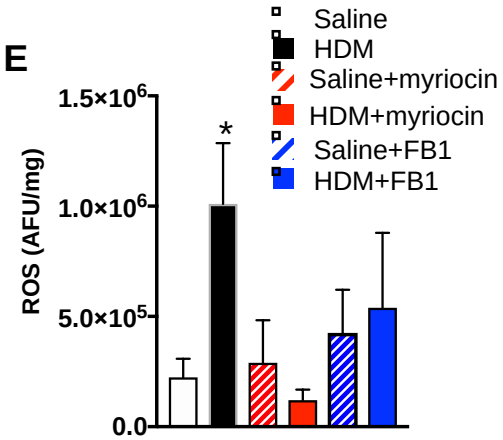
E
Saline
HDM
Saline+myriocin
HDM+myriocin
Saline+FB1
HDM+FB1
ROS (AFU/mg)
1.5×10^6
1.0×10^6
5.0×10^5
0.0
*

Figure 5

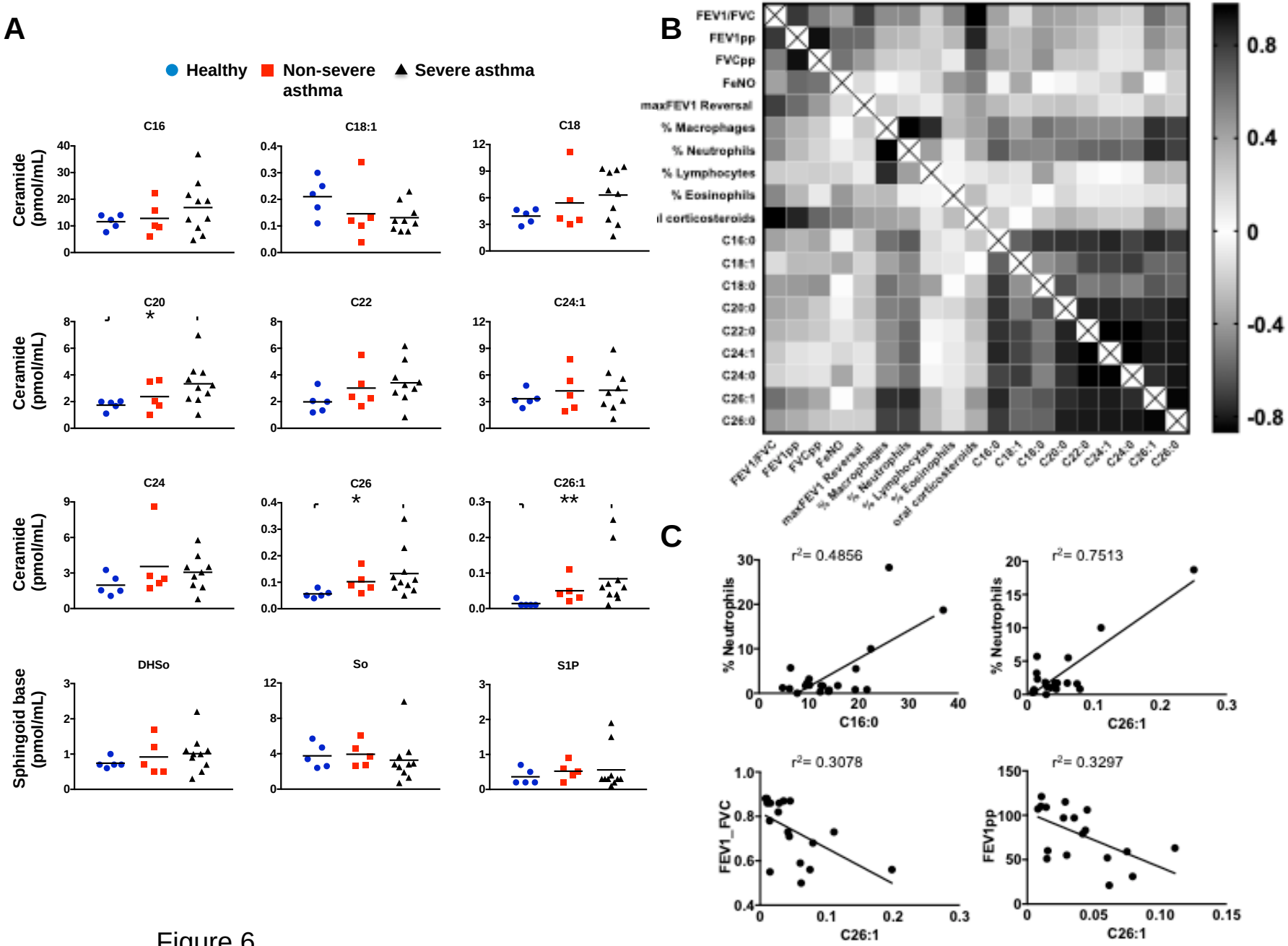
A
Healthy
Non-severe asthma
Severe asthma
C16
C18:1
C18
C20
C22
C24:1
C24
C26
C26:1
DHSo
So
S1P
Ceramide (pmol/mL)
Sphingoid base (pmol/mL)
B
FEV1/FVC
FEV1pp
FVCpp
FeNO
maxFEV1 Reversal
% Macrophages
% Neutrophils
% Lymphocytes
% Eosinophils
oral corticosteroids
C16:0
C18:1
C18:0
C20:0
C22:0
C24:1
C24:0
C26:1
C26:0
C
r²= 0.4856
% Neutrophils
C16:0
r²= 0.7513
% Neutrophils
C26:1
r²= 0.3078
FEV1_FVC
C26:1
r²= 0.3297
FEV1pp
C26:1

Figure 6

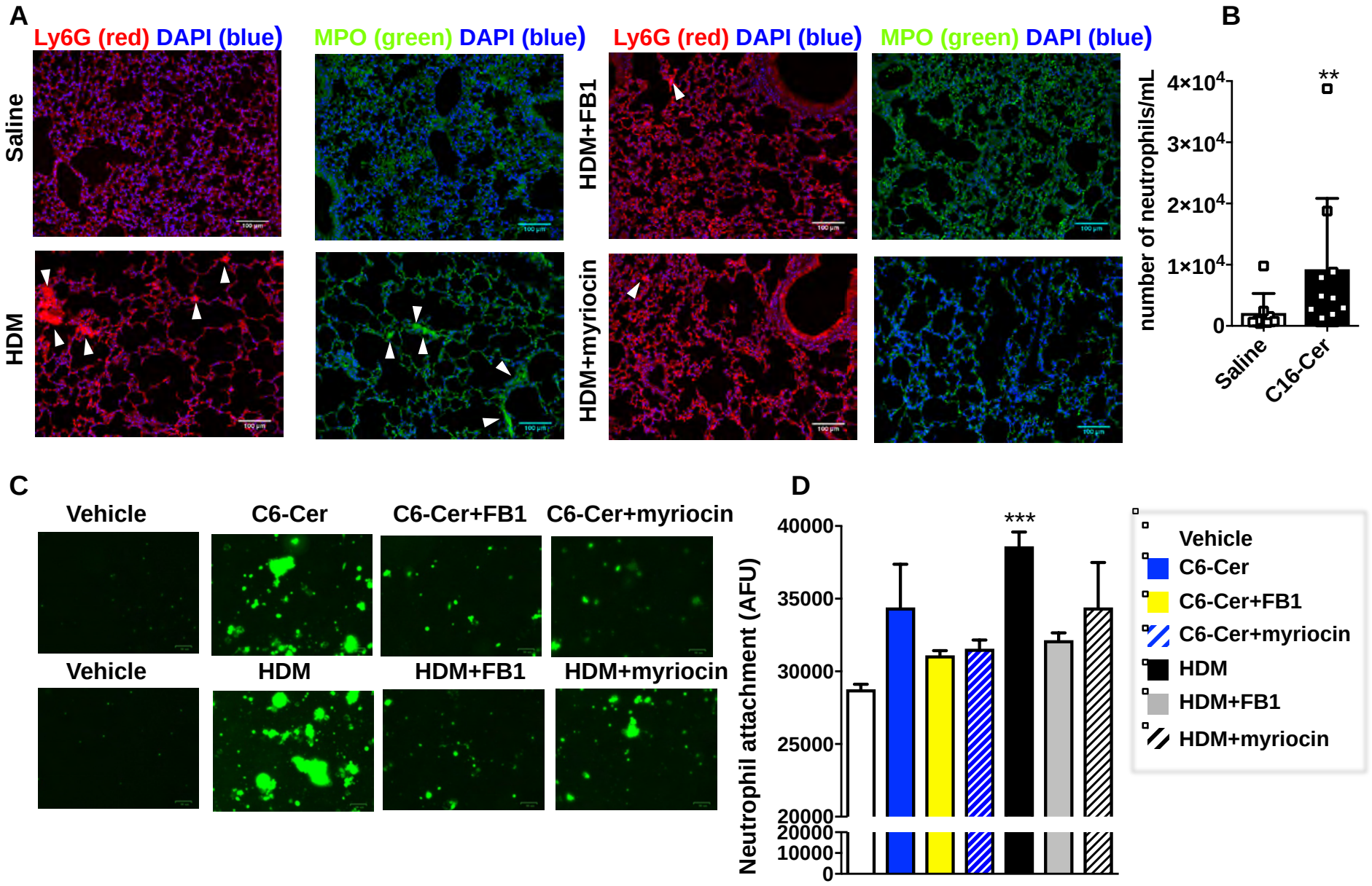
A
Ly6G (red) DAPI (blue)
MPO (green) DAPI (blue)
Ly6G (red) DAPI (blue)
MPO (green) DAPI (blue)
Saline
HDM
HDM+FB1
HDM+myriocin
B
number of neutrophils/mL
4×10^4
3×10^4
2×10^4
1×10^4
0
**
Saline
C16-Cer
C
Vehicle
C6-Cer
C6-Cer+FB1
C6-Cer+myriocin
Vehicle
HDM
HDM+FB1
HDM+myriocin
D
Neutrophil attachment (AFU)
40000
35000
30000
25000
20000
20000
10000
0
***
Vehicle
C6-Cer
C6-Cer+FB1
C6-Cer+myriocin
HDM
HDM+FB1
HDM+myriocin

Figure 7

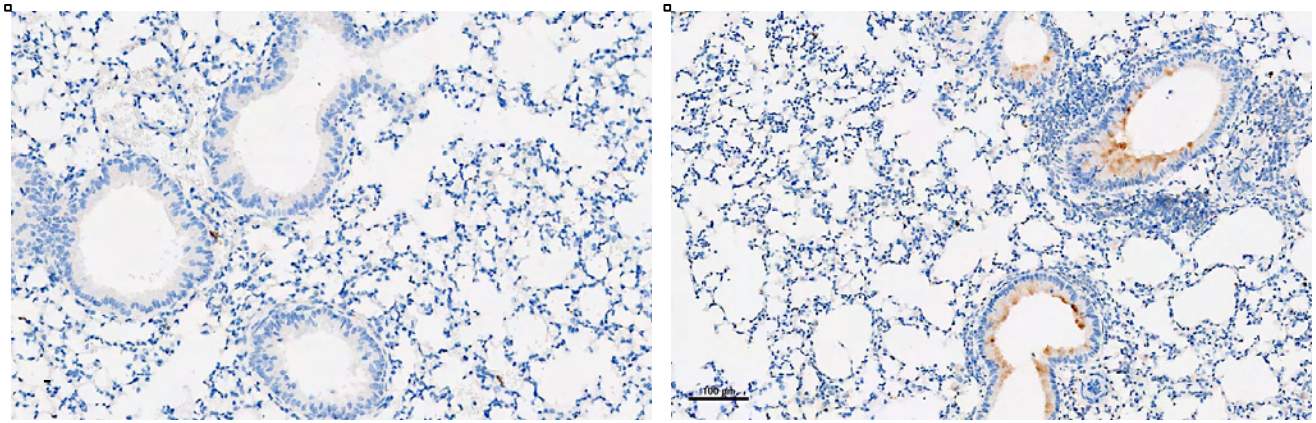

**Saline** **HDM**

**Figure E1**

A

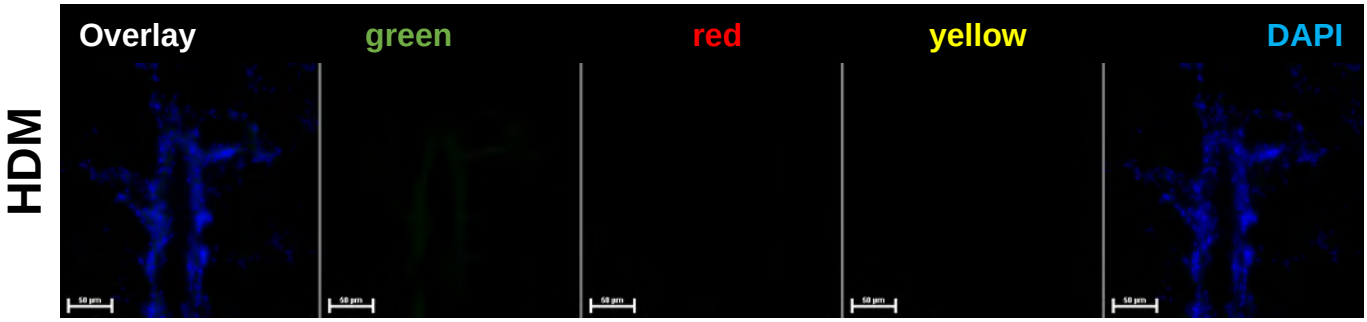


Figure E2

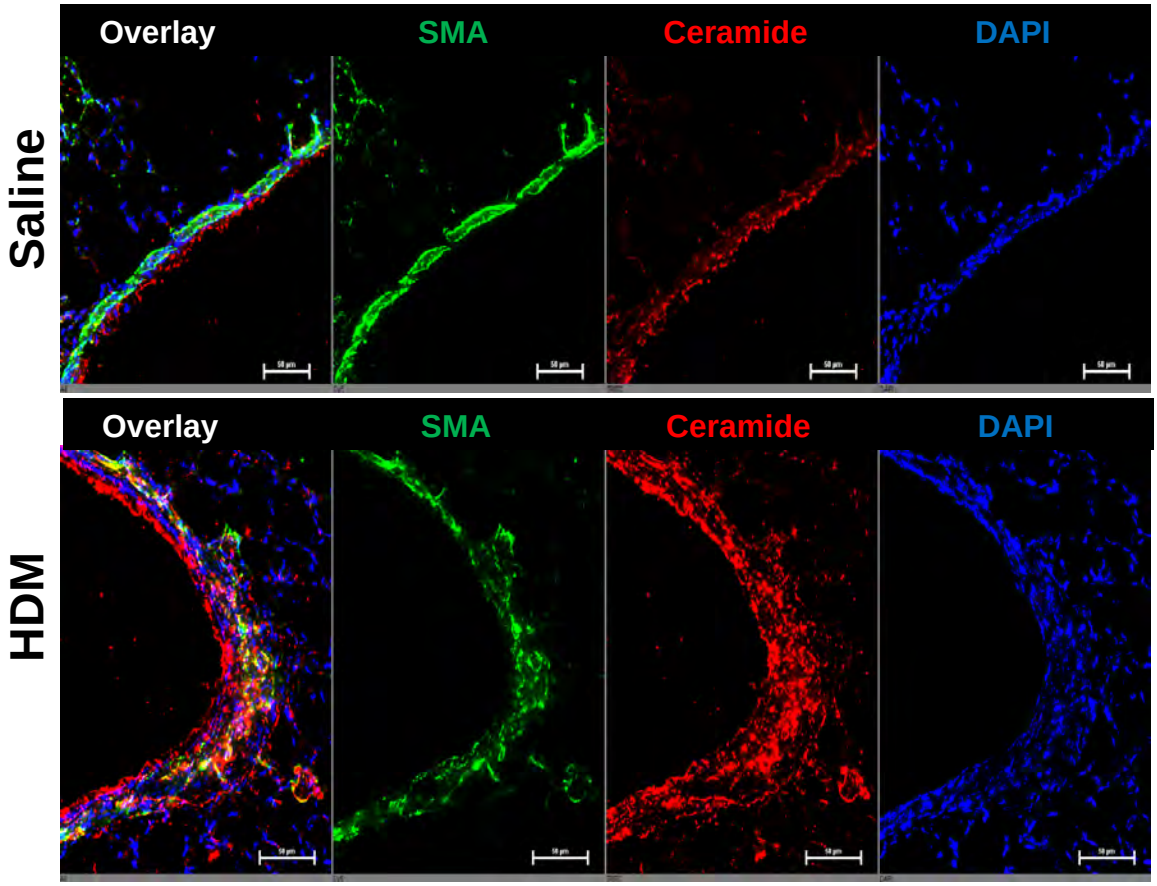
Overlay
SMA
Ceramide
DAPI
Saline
Overlay
SMA
Ceramide
DAPI
HDM

**Figure E3**

## HDM

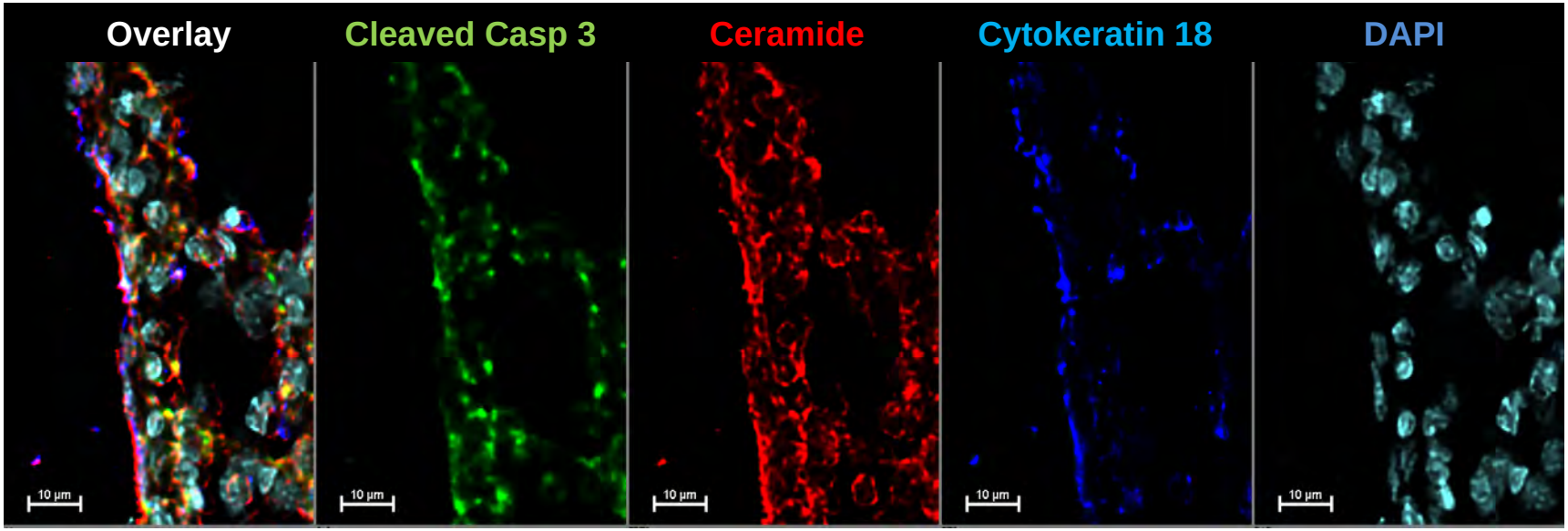


Figure E4

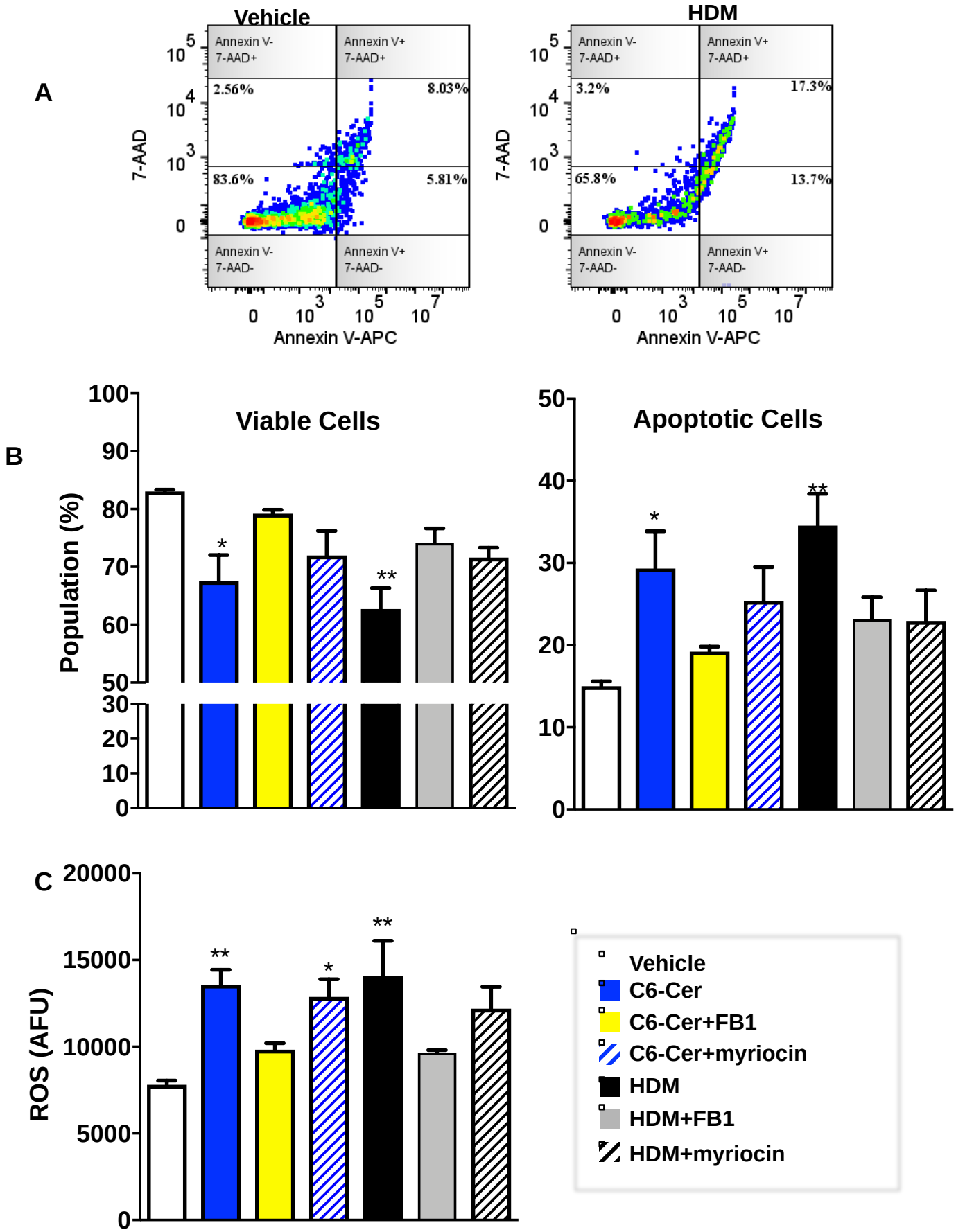
A
Vehicle
HDM
Annexin V-
7-AAD+
Annexin V+
7-AAD+
Annexin V-
7-AAD-
Annexin V+
7-AAD-
2.56%
8.03%
83.6%
5.81%
3.2%
17.3%
65.8%
13.7%
7-AAD
Annexin V-APC
B
Viable Cells
Apoptotic Cells
Population (%)
C
ROS (AFU)
Vehicle
C6-Cer
C6-Cer+FB1
C6-Cer+myriocin
HDM
HDM+FB1
HDM+myriocin

Figure E6

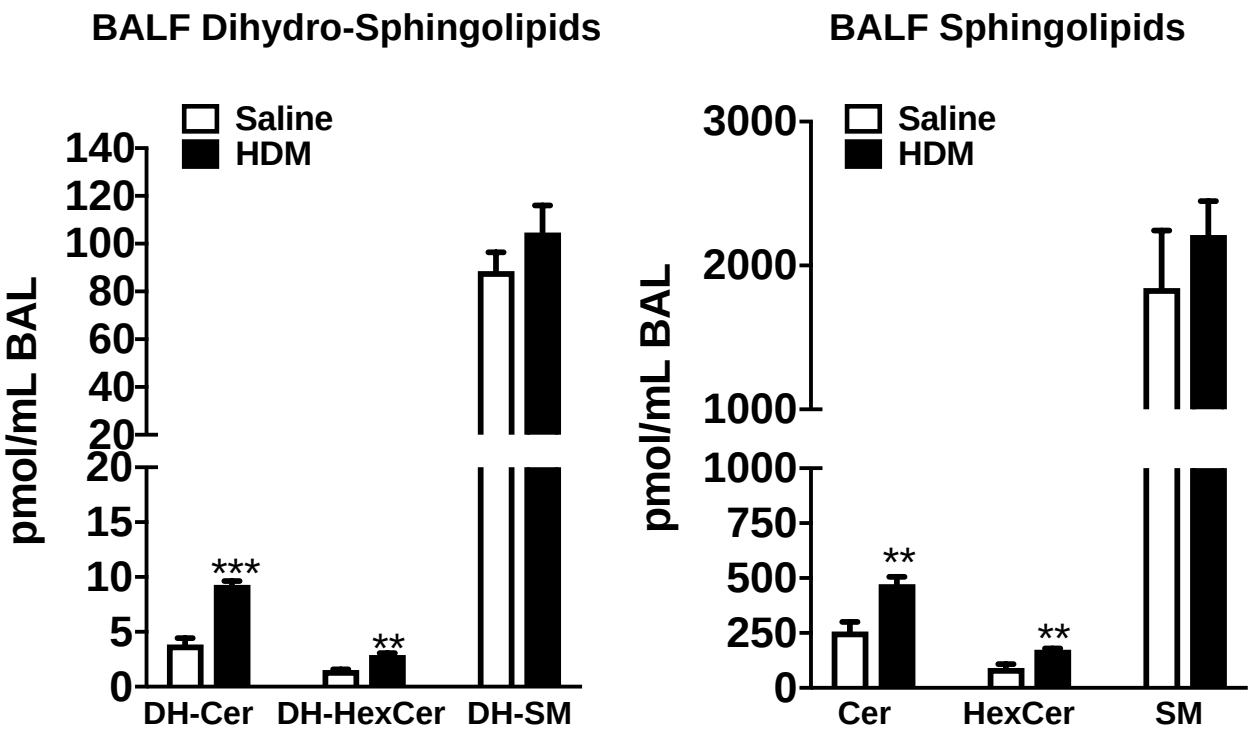
BALF Dihydro-Sphingolipids
Saline
HDM
pmol/mL BAL
140
120
100
80
60
40
20
20
15
10
5
0
***
**
DH-Cer
DH-HexCer
DH-SM
BALF Sphingolipids
Saline
HDM
pmol/mL BAL
3000
2000
1000
1000
750
500
250
0
**
**
Cer
HexCer
SM

Figure E5

# Allergen-induced ceramide elevation leads to cell death, oxidative stress, and neutrophil infiltration in allergic asthma

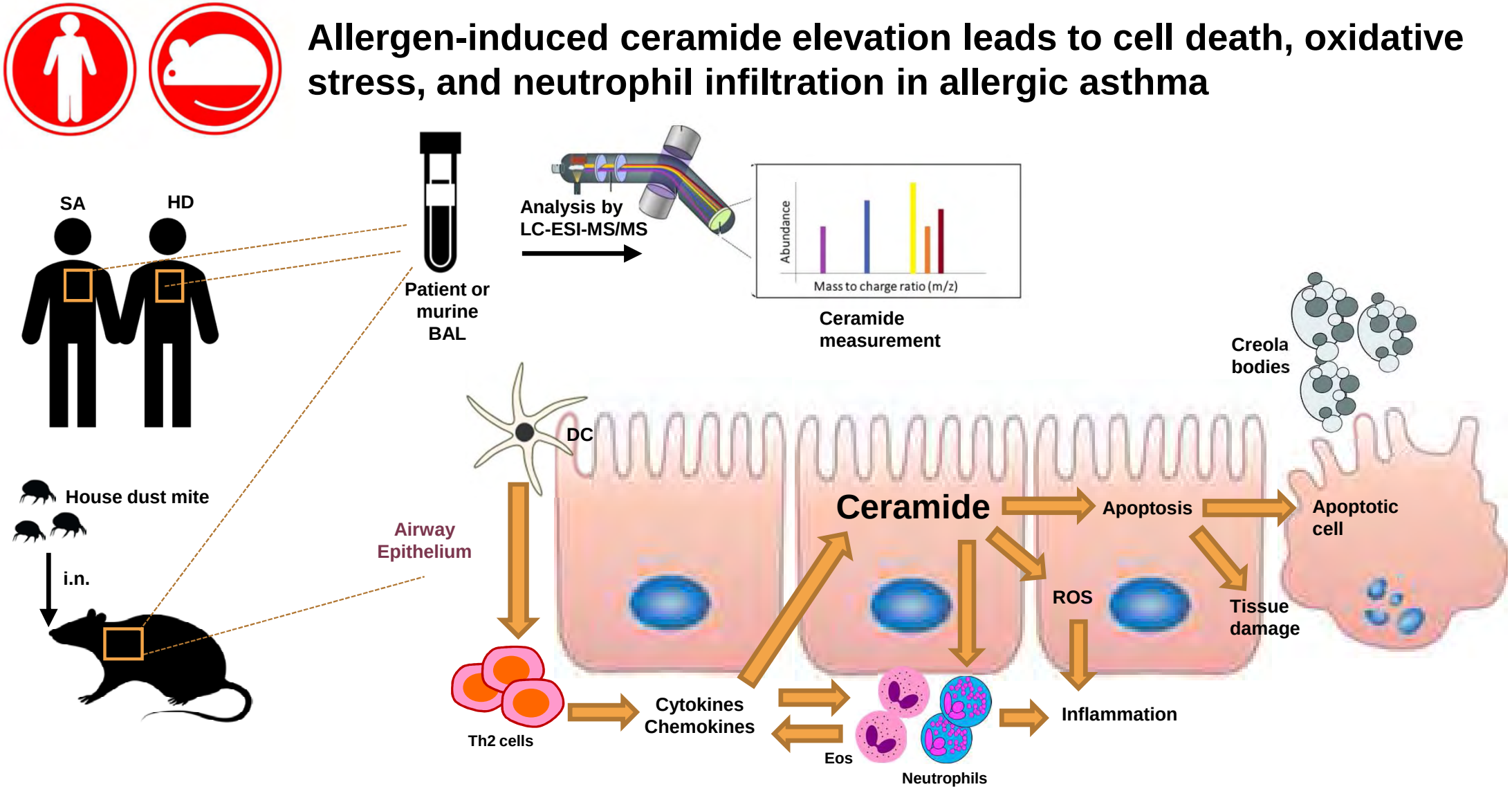


**Abbreviations**

i.n. : intranasal injection; SA: severe asthma; HD: healthy donors; BAL: broncholoalveolar lavage; LC-ESI-MS/MS: liquid chromatography electrospray ionization-tandem mass spectrometry; DC: dendritic cells; Th2: T helper 2 cells; Eos: eosinophils; ROS: reactive oxygen species

The Journal of Allergy & Clinical Immunology
JACI